PRINCETON UNIVERSITY

MENT OF AERONAUTICAL ENGINEERING

A STUDY OF PILOT INDUCED
LATERAL-DIRECTIONAL INSTABILITIES

R. L. Caporali
J. P. Lamers, Lieutenant, USN
J. R. Totten, Major, USAF

Aeronautical Engineering Report No. 604

May 1962

Submitted in partial fulfillment of the requirements for the degree of Master of Science in Engineering from Princeton University, June, 1962.

ACKNOWLEDGEMENTS

The authors wish to express their appreciation to Professor Edward Seckel of the Princeton University Aeronautical Engineering faculty for his assistance and guidance throughout this investigation.

Appreciation is also expressed to Mr. David Ellis for his piloting assistance and to the hangar personnel for their technical support.

TABLE OF CONTENTS

PAGE NUMBER

LIST OF TABLES

LIST OF FIGURES

LIST OF FIGURES (continued)

DEFINITION OF SYMBOLS

b - Wing span - ft

C_L - Lift coefficient

C_l - Rolling moment coefficient

C_n - Yawing moment coefficient

C_y - Side force coefficient

C_{l_r} - Roll due to yaw - $\partial C_l / \partial \left(\frac{rb}{2V} \right)$

C_{l_p} - Damping in roll - $\partial C_l / \partial \left(\frac{pb}{2V} \right)$

C_{n_r} - Damping in yaw - $\partial C_n / \partial \left(\frac{rb}{2V} \right)$

C_{n_p} - Yaw due to roll - $\partial C_n / \partial \left(\frac{pb}{2V} \right)$

d - Indicates differentation with respect to τ time: $\frac{d(\ )}{d(t/\tau)}$

J_x - Non-dimensional moment of inertia about the x principal axis

J_z - Non-dimensional moment of inertia about the z principal axis

K - Gain of pilot

k - Radius of gyration - ft

k_i - Potentiometer gain constant $i = 1,2,3 \ldots n$

M - Mach number

DEFINITION OF SYMBOLS (continued)

p - Roll rate, deg/sec or radians/sec

q - Dynamic pressure - psf

r - Yaw rate, deg/sec or radians/sec

s - Laplace transform variable

t - Time - sec

V - Steady state velocity - ft per sec

α_o - Trim angle of attack of principal axis, radians

β - Sideslip angle - deg or radians

δ_a - Aileron deflection - radians or degrees

ζ_ϕ - Damping ratio of the approximate Dutch roll mode depicted by the denominator term of the "pilot gain" root locus equation

ζ_ψ - Damping ratio of short period Dutch roll mode

λ - A root of the characteristic equation (Subscript s refers to spiral root and subscript r refers to roll root)

μ - Airplane density factor - $m/\rho S b$

ρ - Density of air - slugs/ft^3

τ - Time parameter $\frac{m}{\rho S V}$ - sec

ϕ - Roll angle - deg or radians

ψ - Yaw angle - deg or radians

DEFINITION OF SYMBOLS (concluded)

$\omega_{n\phi}$ -	Undamped natural frequency of approximate Dutch roll mode depicted by the denominator term of the "pilot gain" root locus equations - radians/sec
$\omega_{n\psi}$ -	Undamped natural frequency of the short period Dutch roll mode - radians/sec

Subscripts:

1. The subscripts β , and δ_a indicate the partial derivative of the coefficient with respect to the specific subscript.
2. The subscripts x and z indicate reference axis.
3. A dot above a variable indicates a derivative with respect to time.

Other terms or symbols are explained where introduced.

ABSTRACT

A physical description of the destabilizing mechanism responsible for certain pilot induced lateral-directional instabilities is included herein. In addition, the theoretical and experimental effort proporting to support the physical arguments is included.

The basis for this study was a pilot induced instability known to exist for the X-15 research aircraft-pilot combination for certain conditions of flight. Accordingly, a major portion of the effort was concentrated upon the analysis of a specific known instability. Nevertheless, it is the opinion of the authors that the resultant conclusions are quite general.

SECTION I

INTRODUCTION

The investigation upon which this report is based was concerned with the study of a type of pilot induced instability of the lateral-directional short period mode.

In the more usual case, an instability of this nature can be explained as a function of the characteristic response time of a human being, in which case the problem is quite simply that the human controller cannot react to the error signals with sufficient speed. Quite obviously, a problem of this nature is closely related to the frequency of the mode of motion.

Some recent studies, however, have indicated the possibility that certain pilot induced - or closed loop - instabilities can occur which do not appear to be strictly a function of frequency. A study by Askenas and McRuer, (Ref. 1) based upon root locus analyses of a pilot-airplane combination, showed the possibility of an instability of this type. This study further indicated certain combinations of the aerodynamic stability derivatives believed to be unfavorable.

More recently, an analysis was made by Taylor (Ref. 2) as a result of simulator studies of the X-15 research aircraft. These simulator studies predicted

certain flight condition boundaries within which the X-15 closed loop system would exhibit an unstable lateral directional short period mode. (Dutch roll mode). That this region did in fact exist was verified by flight tests.

Both of these studies relied heavily on the root locus technique for an explanation of how the magnitude of pilot initiated control movements could destabilize an otherwise stable system. Consequently, although the studies showed that the pilot could destabilize the system, the actual destabilizing mechanism was not explained. This study was initiated in an effort to provide this explanation.

This study was conducted in three separate, yet complementary, phases. The theoretical phase consisted of an examination of the basic equations of motion and the significance of certain parameters upon the resultant dynamic behavior or a given pilot-airplane system. Root locus analyses formed a major portion of this phase.

What has been called the computer-simulator phase was essentially a study of the same parameters investigated theoretically, but with the aid of an electronic analog computer. In addition, the analog computer was used as a fixed base simulator for the investigation of an actual closed-loop system.

The flight phase consisted of flight tests incorporating the variable stability NAvion aircraft described herein. This phase was primarily initiated in an effort to provide as realistic a simulation as possible of an unstable pilot-airplane combination.

In general, it may be stated that the results of all three phases contributed significantly to the conclusions which resulted from this investigation.

SECTION II

EQUIPMENT

The variable stability flight simulator used in this investigation was a North American NAvion airplane. To provide the variable stability capability, a modified Minneapolis-Honeywell autopilot, USAF Type E-12, had been installed. Modifications to the autopilot consisted of the addition of supplementary rate gyros and a sideslip transducer. Signals from the transducers, proportional to the measured quantities, were introduced as input signals to the autopilot, resulting in control deflections proportional to the measured quantity. This made the system capable of modifying the airplane stability derivatives. Data collection and recording were accomplished by means of an ASCOP pulse width, frequency modulated telemetering system. An analog computer was used in the theoretical development of the problem, and, in conjunction with a control stick-operated potentiometer, provided fixed-base simulation.

TEST AIRPLANE

The NAvion is an all metal, low wing, single-engined monoplane. The engine, a Continental E-185, drives a variable pitch Hartzel propeller and is rated at 185 horsepower - maximum continuous at sea level at 2300 rpm. The control surfaces are of conventional design. A

streamlined static balance is fixed at the outboard end of each aileron. The trim tabs for the aileron and rudder are of the fixed-bend type, and the elevator trim tab is adjustable from the cockpit. The physical characteristics of the NAvion are listed in Table I. A photograph of the test airplane is shown in Fig. 1. The airplane was equipped for this investigation with a three-axis variable feedback autopilot.

AUTOPILOT

The basic autopilot is capable of altering the stability of the airplane in the pitch, roll and yaw axes through three channels of operation. For this investigation, the pitch channel was rendered inoperative, with the exception of an unmodified elevator control. Each channel is composed of an AC series summing network which combines signal voltages from the sensing transducers, the electrical flight controls and the knob actuated trim controller. The difference between this combined signal voltage and a voltage feedback signal from the servo-drum position transducer, an error signal, is applied to an amplifier, phase discriminated and transferred into servo drum rotation by means of dual power relays. The servo drum rotation moves the control system of the aircraft. The motion of

Fig. 1
NAvion Test Airplane

the control surface continues until error signal voltage at the input to the amplifier is reduced to a value below the threshold of the system. This value is about fifty millivolts.

The basic autopilot had been modified by deleting some of the original provisions and by supplying additional feedback loops. The directional coupler feedback loop, the flight control stick trim provisions, and the coordinated turn provisions had been eliminated. Sideslip angle and roll rate feedback loops and a cross-control signal proportional to aileron control stick deflection had been added to the yaw channel. Sideslip angle and yaw rate feedback loops had been added to the roll channel. The manually adjustable ratio potentiometers were relocated on a gain control panel placed between the pilots' seats. An electronic safety device was installed to prevent "hard-over" signals by automatically disengaging the autopilot if an error voltage exceeding approximately 3 volts should instantaneously appear at the amplifier input.

Quantities to be telemetered were taken from the appropriate terminals on the main terminal board to a 15 channel filter-conversion unit which converted the voltage to DC. A gain control for each channel permitted the DC voltage to be adjusted to that required by the telemetering system (0-5 volts). From the filter-conversion

unit, the DC voltages representing the measured quantities were taken to an auxiliary terminal strip and connected to the telemeter transmitter unit.

The electrical controls are located in the right seat of the NAvion, and the standard manual controls in the left seat. Reference 3 described a spring centering device and fluid dashpots which had been incorporated in the electric stick. These had provided objectionable feel characteristics and, according to the recommendations in Reference 3, were removed prior to the flight test phase of this investigation.

INSTRUMENTATION

The transducers in the feedback loops of the modified autopilot provided signals to the autopilot amplifier through the AC summing networks and provided the signals required to measure the aircraft motions. The flight condition data (airspeed, altitude, and outside air temperature) were obtained from standard aircraft instruments. Errors in these instruments were assumed negligible. The physical characteristics of the components of the instrumentation system are listed in Table II.

Two of the modified rate gyros were located on the autopilot chassis on the main equipment table and two were mounted on the floor of the aircraft in the equipment compartment.

The use of a single sideslip vane was possible because it contained two separate potentiometers. The sideslip vane was installed on a boom extending four feet ahead of the wing leading edge at the wing tip. It was assumed that this distance was adequate to minimize measurement errors due to the wing pressure field. The position of the sideslip vane was such that the yawing rate of the aircraft about the vertical body axis would affect the sideslip angle measurement slightly, but this effect was neglected.

The telemeter transmitter unit consists of a rotary switch sampling each of 43 input channels plus two synchronizing channels at the rate of 20 times per second. The sampled data are converted to pulse width form by a keyer unit and transmitted as a UHF frequency modulated signal to the telemeter ground station. The filter-conversion unit limited the data measurements to 14 quantities plus a full scale reference voltage. By jumper wiring on the auxiliary telemetering terminal strip it was possible to sample a given quantity more than once for each revolution of the switch. Specifications of the telemeter transmitter unit are listed in Table II.

GROUND STATION

The ground station data collection equipment consisted of an ASCOP M series PW/FM ground station, an

Ampex Model 309C dual track tape recorder and associated graphical recorders.

The ASCOP ground station received the modulated signals from the airborne unit, demodulated and decoded the signals to provide for each of the 43 channels of information, and provided a continuous voltage output to the recorders representing the measured flight data.

The tape recorder had provisions for simultaneous recording of telemeter and voice transmissions. This permitted the recording of description of runs, pilot's comments and ground station operator's comments along with the telemeter data.

Sanborn four channel pen recorders, Model 154-100B, were used in the graphical recording phases.

ANALOG COMPUTER

The analog computer used in this investigation was a Goodyear Aircraft Corporation Model L3 (GEDA) linear electronic differential analyzer. Twenty-four automatically stabilized DC computing amplifiers were available with open-loop gain greater than 5×10^7, and of negligible drift. The computer incorporated an automatic error indicator and had a guaranteed accuracy of one percent. Provisions were available for accurately setting computer board potentiometers by the use of a special calibration potentiometer and null indicator.

Attempts to "fly" the computer were conducted by means of the simulator shown in Figure 2. This consisted of a conventional control stick which, when deflected, varied the voltage at the δ_a terminals of the analog computer circuit by changing the setting of a potentiometer.

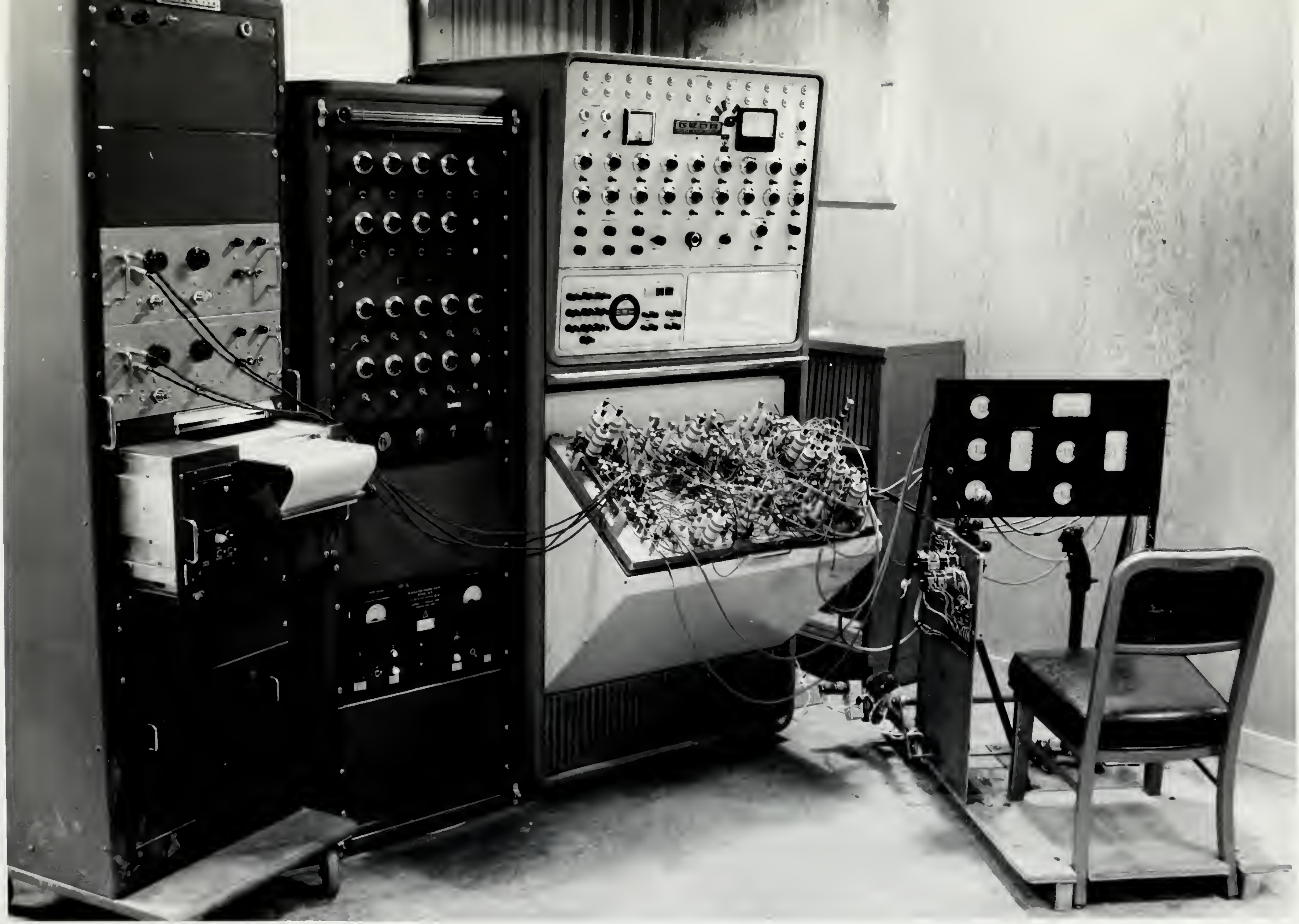

Fig. 2

Analog Computer - Simulator

SECTION III

PROCEDURE

A. In-Flight Simulation

In-flight simulation of the pilot induced lateral-directional oscillation was accomplished with the variable stability NAvion. It was expected that results obtained in this manner would provide a more suitable basis for a physical explanation of the phenomenon than results obtained from a fixed base simulator, since the full range of visual and kinesthetic motion cues would be present.

Reference 2 points out uncontrollable combinations of Mach number and angle of attack encountered with the X-15 research aircraft with lateral stability augmentation off and the pilot attempting to control bank angle in a normal manner with ailerons alone. Using these conditions as a guide, values were obtained for the dimensional stability derivatives to be reproduced in the NAvion. These are listed in Table III. The calculation procedure is shown in Appendix A. These derivatives were dimensionalized for a dynamic pressure of 153 lbs./ft.^{2}, corresponding to one g flight. This choice of a relatively low dynamic pressure was made in order that the capabilities of the autopilot/airplane system not be exceeded; it was anticipated that the

frequency of the Dutch roll oscillations would be reduced, while the character of the pilot-induced instability would be retained. Simulation at higher dynamic pressure was confined to the fixed base simulator.

Dimensional derivatives for the NAvion were obtained for 6500 ft. standard density altitude and 120 miles per hour true airspeed (Ref. 4). Autopilot feedback gain constants were then determined **which** would alter these derivatives, making them equal to those chosen as typical for the X-15. This procedure is shown in Appendix **A**.

Feedback gain constants of the autopilot could be altered by adjustment of potentiometer settings in the cockpit of the NAvion. In order to determine gain potentiometer settings which would provide the required constants it was necessary to calibrate the system.

Each autopilot rate gyro was calibrated by removing it from the airplane and remounting it on an electrically driven turntable which could be rotated at a controllable rate. In this manner control surface deflections produced by given angular velocities could be established. The deflections were measured by a propeller protractor for various gain potentiometer settings.

The sideslip vane was calibrated by moving it through a specified angle and simultaneously measuring the control

surface deflections produced at different gain potentiometer settings. Electric stick calibration was obtained in the same manner, a propeller protractor being used to measure stick deflection.

The results of the calibration are shown in Figure 3, as curves of Feedback Gain Constant versus Gain Potentiometer Faceplate Setting. The numbering of the constants corresponds to the number of the potentiometer by means of which each may be adjusted. The cockpit panel arrangement is shown in Figure 4.

In order that a quantitative interpretation of the telemetered motion histories of the aircraft could be made, it was also necessary to calibrate the system for telemetry. This was performed in exactly the same manner as the calibration described above, with the exception that the measured output quantity in this case was voltage at the telemetry transmitter package, rather than control surface deflection. It was decided that the following quantities would provide sufficient information for the analysis to be performed: roll rate, yaw rate, stick deflection and sideslip angle. The results of the telemetry calibration are shown in Figure 5 as curves of the foregoing quantities versus Telemetry Input Voltage.

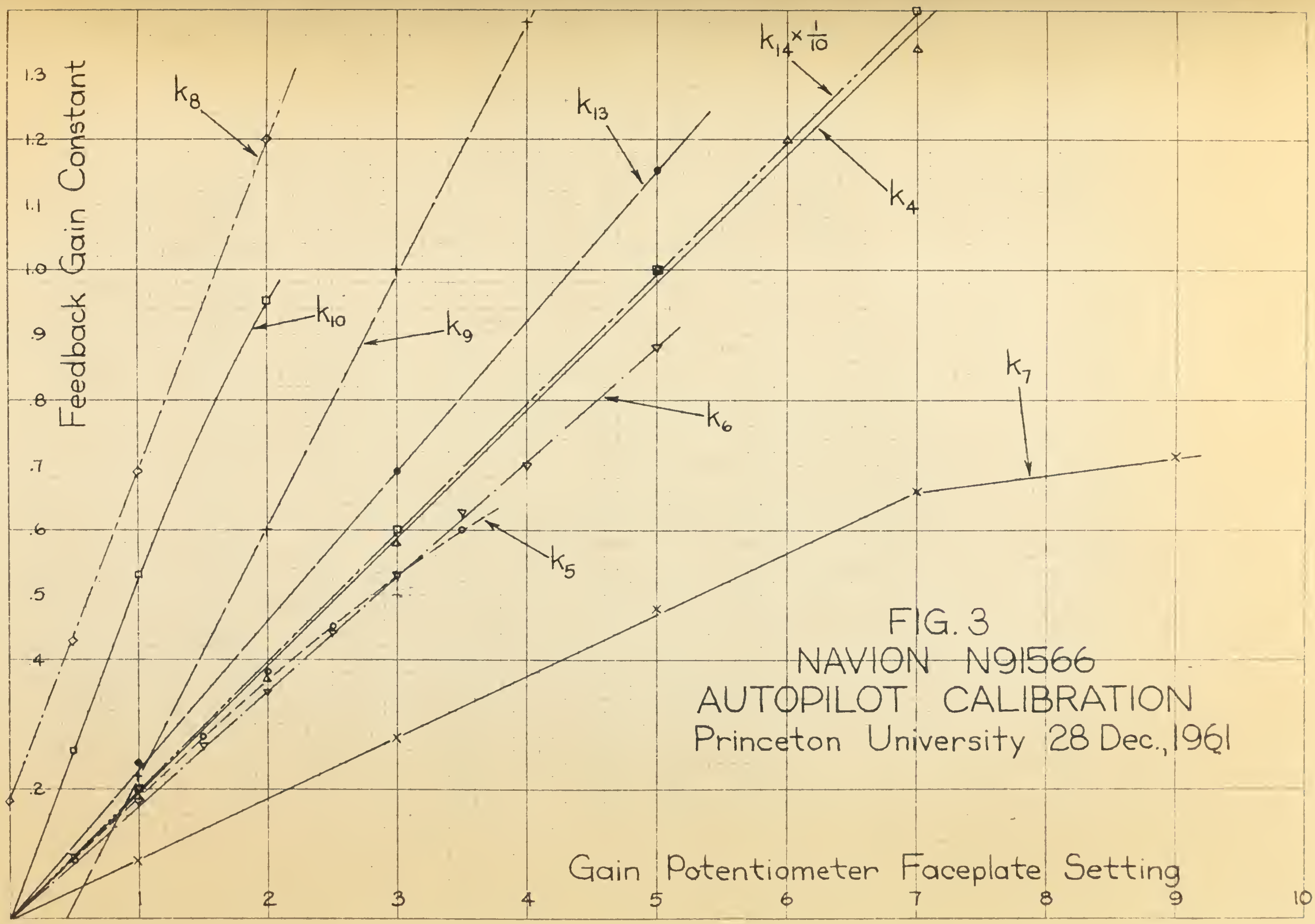

FIG. 3
NAVION N91566
AUTOPILOT CALIBRATION
Princeton University 28 Dec., 1961

FIG. 4
NAVION N91566
COCKPIT POTENTIOMETER PANEL

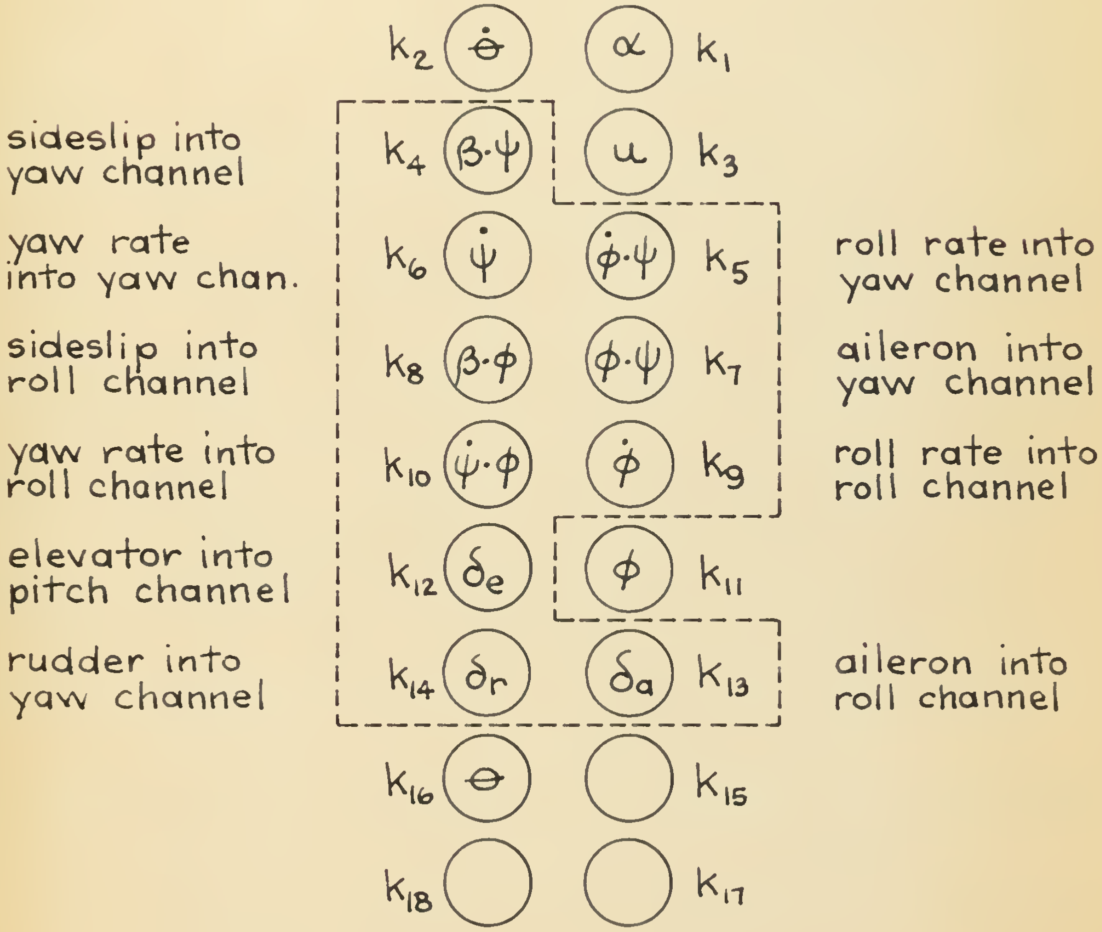

note: feedbacks utilized in this investigation are enclosed by dashed line

FIG. 5

TELEMETRY CALIBRATION

Princeton Univ., 26 Jan., 1962

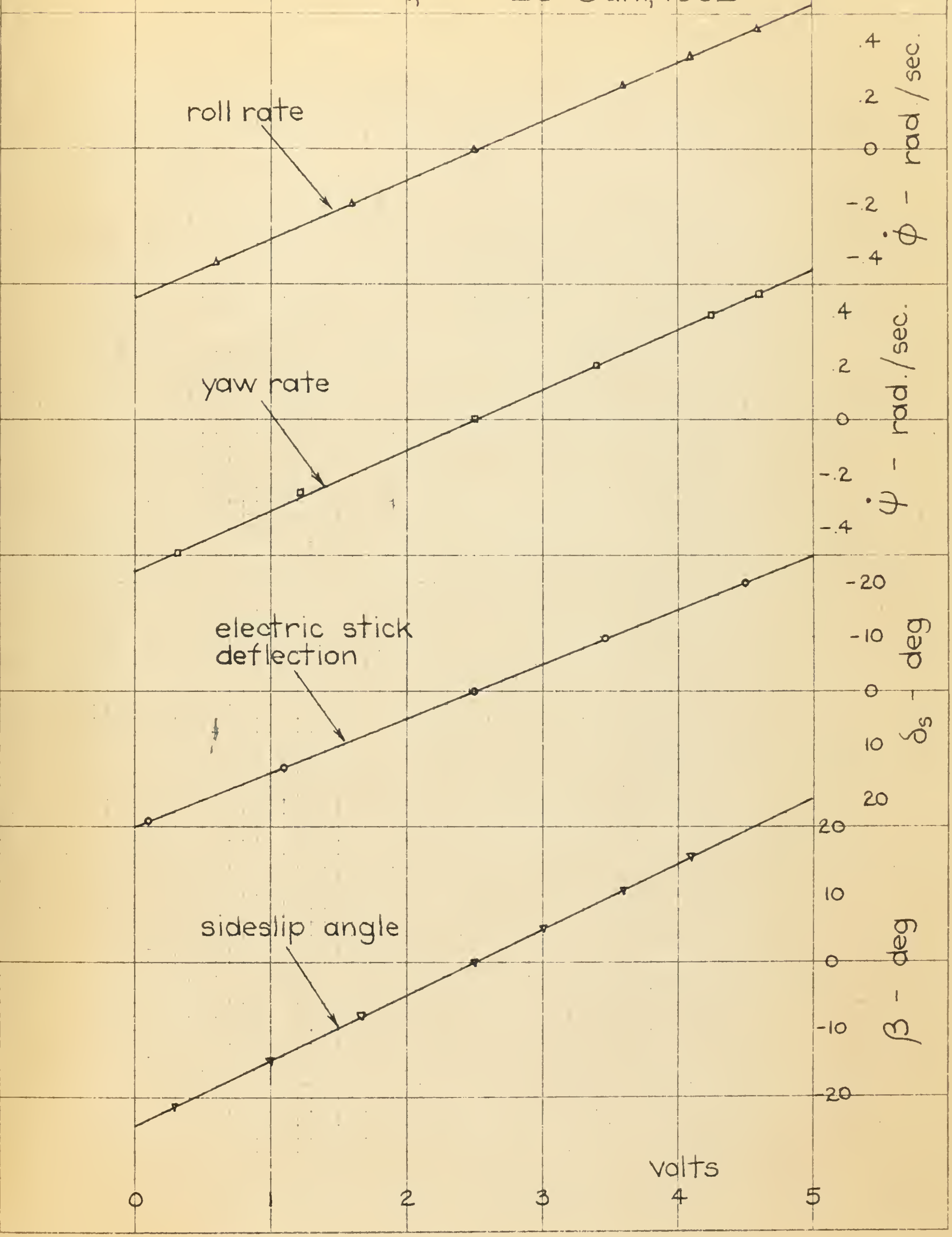

Longitudinal feedbacks, (pitch angle, pitch rate, velocity and angle of attack) were not employed in this investigation. The elevator gain potentiometer was adjusted to a value which gave a satisfactory elevator response.

Certain deficiencies existed in the equipment which made it difficult to achieve an exact simulation. Among these were control cable stretch, structural elasticity of the aircraft, inaccurate resolution due to finite autopilot "peck sizes," very small potentiometer settings and the difficulty of accurately reproducing a potentiometer setting. As a result of these deficiencies it was found that the simulation procedure outlined in this section provided only a first approximation to the desired aircraft response. It was necessary, therefore, to further adjust the cockpit gain potentiometer settings in order to achieve the desired results.

This arbitrary correction to the calculated potentiometer settings would necessitate matching of aircraft responses to analog computer responses if the objective was exact simulation. A reasonably good qualitative simulation of such motions can be readily achieved, however, and was considered to be sufficient for the purpose of this investigation.

B. Analog Computer Study

Three basic tools were used to accomplish the computer phase of this investigation. These were:

1. the GEDA Analog Computer,
2. the Sanborn Recorder, and
3. the Control Stick Simulator.

The computer and recorder were used to do the open loop studies of the system, while all three units were used to complete the closed loop work.

The equations mechanized in the computer are listed and discussed in detail later in this report.

When open loop response to step inputs by the computer matched calculated values as to time to damp to 1/2 amplitude and period of oscillation, attempts were made to "fly" the computer. These closed loop trials were accomplished by using the control stick simulator in the same manner as the control stick in an aircraft. The time histories of bank angle, roll rate, sideslip angle, and yaw rate on the recorder were used as references. The control stick simulator produced input voltages to the computer analogous to aileron inputs to the basic airplane.

Three separate configurations of the basic equations of motion were investigated. These were:

A. $\alpha_0 = 0$ and low dynamic pressure (153 psf).

B. $\alpha_0 = 10°$ and low dynamic pressure (153 psf).

C. $\alpha_0 = 10°$ and high dynamic pressure (1000 psf).

The wiring diagrams for the computer study are shown in Figures 6 and 7.

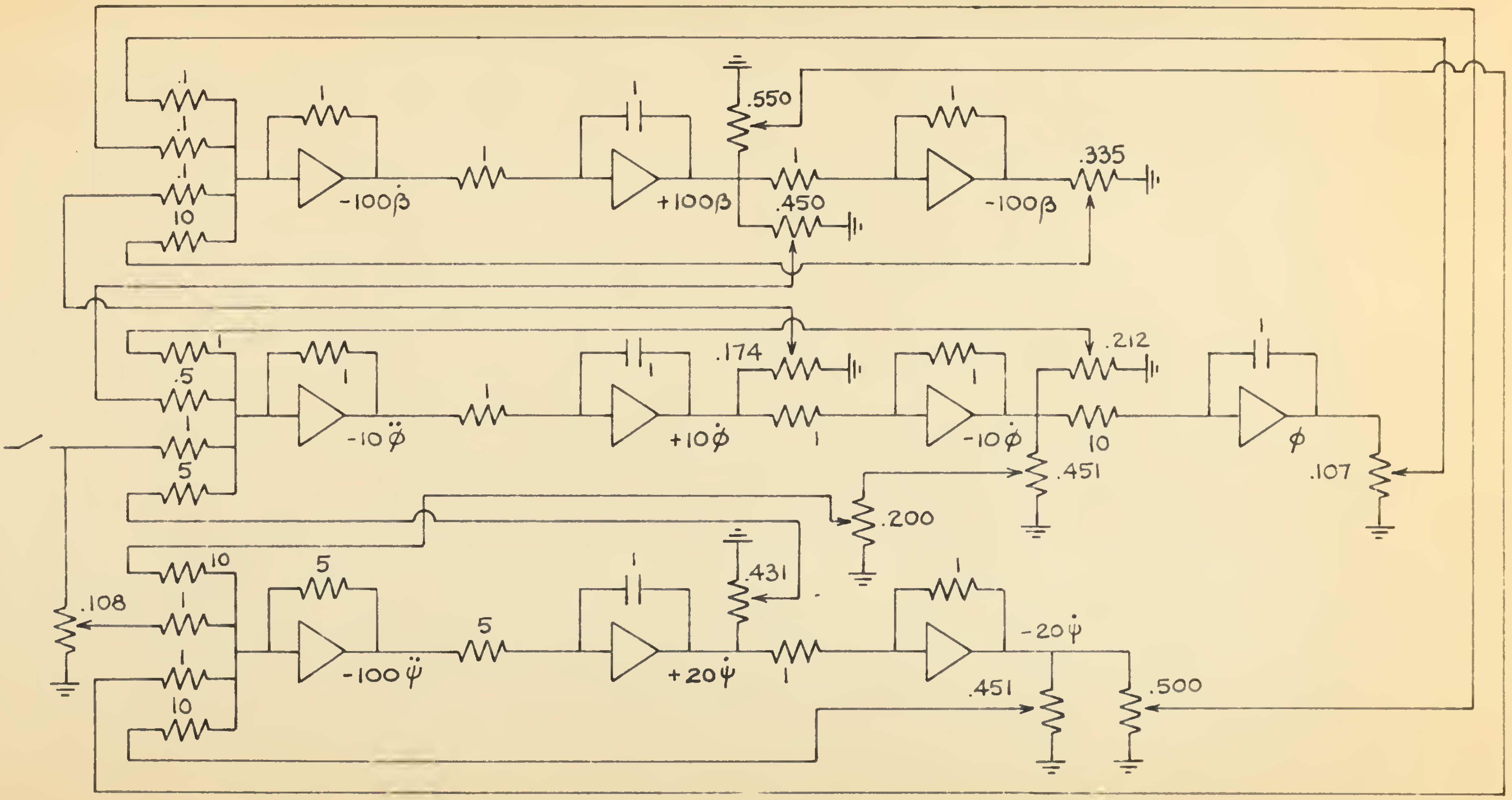

FIG. 6

ANALOG COMPUTER DIAGRAM

Lateral-directional Equations $q = 153$ lb./ft.^{2}

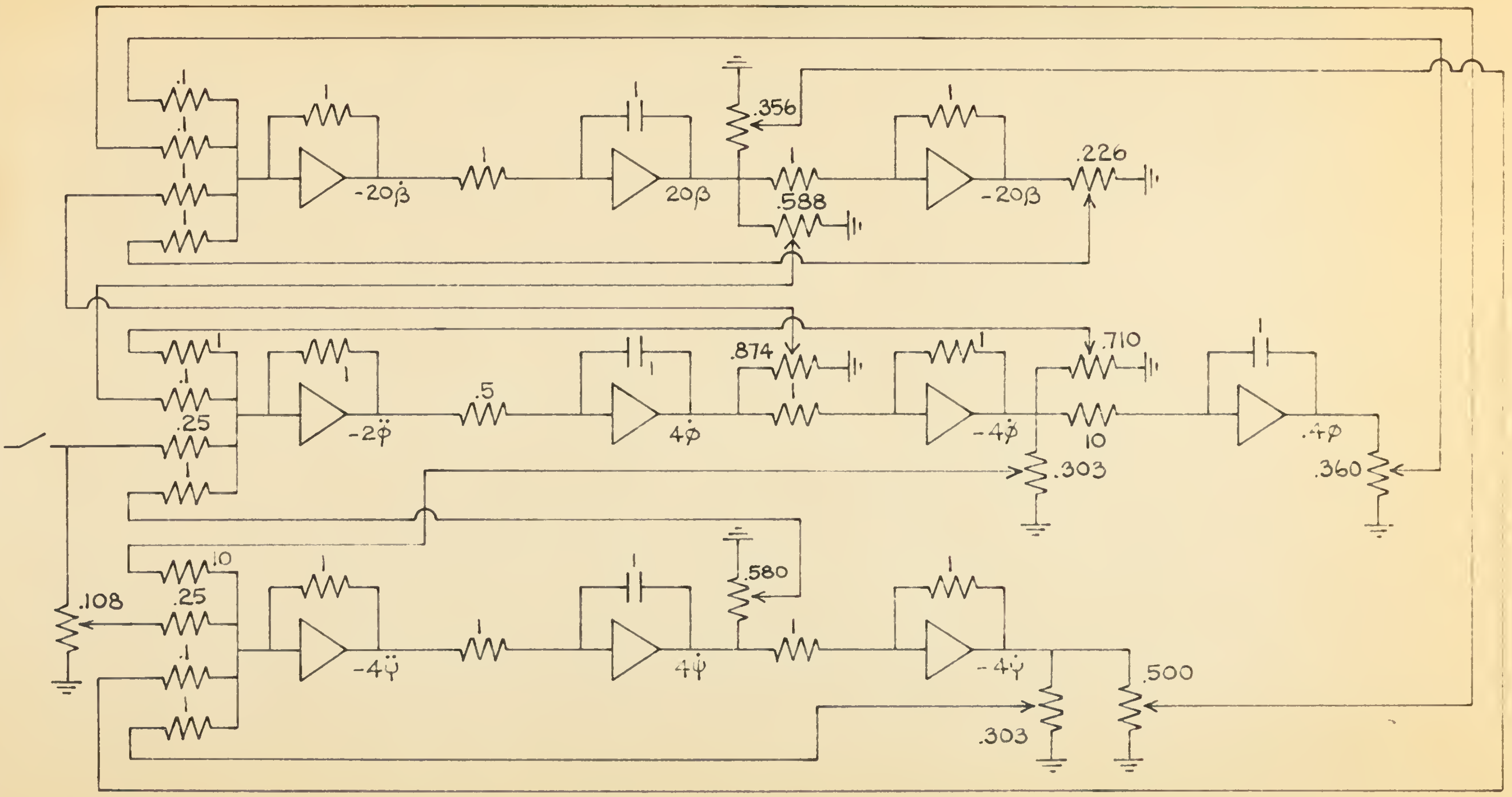

FIG. 7

ANALOG COMPUTER DIAGRAM

Lateral-directional Equations $q = 1000$ lb./ft.^{2}

SECTION IV

DISCUSSION AND RESULTS

Theoretical Development:

During the past several years, considerable emphasis has been placed on the determination of what parameters can best be used to measure the lateral-directional handling qualities of an airplane. As a result, a considerable body of literature has come into being and certain airplane response characteristics have come to be regarded as unfavorable or undesirable from the standpoint of control by a human pilot. (Ref. 1). Primarily as a result of the human pilot being involved as a part of the feedback control loop, investigations of this nature have not been easy to interpret either physically or mathematically.

This particular investigation has been concerned with a rather special segment of the lateral-directional handling qualities problem - specifically the case where the inclusion of a pilot in the control loop has resulted in an unstable Dutch roll oscillation, although the open loop Dutch roll response of the aircraft was known to be stable. In short, this investigation has been concerned with the specific problem of a pilot induced Dutch roll instability.

The problem of a pilot-airplane combination of the nature described above could have been regarded as general

and an overall solution sought. However, it was felt by the authors that a more concentrated effort could be made if the problem were approached from the opposite point of view - namely a detailed theoretical and experimental investigation using, as a guide, a pilot-airplane combination for which the results were known. The reasoning followed was that a detailed study of a particular situation might then yield a theory which could be investigated in a more general sense.

According to Ref. 2, the X-15 research airplane-pilot combination was found to result in an unstable lateral-directional oscillation for certain flight conditions if the stability augmentation system was made inoperative. For this reason, the X-15 airplane-pilot combination was the closed loop system chosen for the detailed study. Specifically, the instability associated with a flight Mach number of 3 and a ten degree angle of attack was investigated.

The fact that the above configuration was the one chosen for study placed several important restrictions upon the problem and thereby upon the resultant conclusions. First, although the above configuration was handled throughout this study as though the aircraft had been in steady flight, in reality the X-15 encountered the above stated flight condition only in transitory flight.

Accordingly, the aerodynamic stability derivatives were continuously changing, with the result being that the pilots of the X-15 were advised to refrain from using the rudder as a control. Therefore, this entire investigation was conducted assuming the ailerons to be the only type of lateral-directional control available , although the effect of using rudder is discussed in the flight phase section of this discussion. A second condition implied by the problem as stated is that the frequency of the oscillation was not a factor. That this must be so can be reasoned by noting that the frequency is more a function of the dynamic pressure than of Mach number, while the instability has been described as being a function of Mach number and angle of attack. Thus, the solution sought was not one dependent upon the inability of a human being to respond with sufficient speed to an error signal. In effect, a suitable explanation to the problem encountered by the X-15 would have to be valid even if the pilot were assumed to respond without a time lag.

The stability derivatives required for a detailed study of the above condition were obtained from Ref. 5 and are listed in Table IV. These derivatives lead to autopilot potentiometer gain constants listed in Table V. It is noteworthy that only two of the stability derivatives

were significantly different from what one might ordinarily expect. Namely, both $C_{n\delta_a}$, (aileron yaw) and $C_{\ell\beta}$ (dihedral effect) had a positive sign. Thus, these two derivatives immediately became suspect and it was expected that a theoretical analysis of the problem would show either one or both of these derivatives to be involved in an explanation of the instability. In this rather special case of a single control, pilot-induced instability, the unusual sign of the aileron yaw became of particular interest.

A proposed theoretical explanation to the problem encountered by the X-15 aircraft was published by Taylor (Ref. 2). In his work, Taylor showed, by root locus techniques, that the Dutch roll mode of an aircraft with the characteristics exhibited by the X-15 could be made unstable if a pilot gain proportional to roll angle and roll rate was included in the feedback loop. According to Taylor, the ratio of ω_ϕ/ω_ψ could be used to define the region where an instability might occur - a ratio greater than one being indicative of an unfavorable condition. The human transfer function used by Taylor in his analysis was determined empirically and found to be $K(1 + .57s)$. Thus a pilot response proportional to both roll angle and roll rate was assumed. The analysis followed by Taylor was quite believable for two reasons.

First, the transfer function was seen to be independent of a pilot time lag which would seem to isolate any effect of frequency from the basic control problem. Secondly, the analysis as carried forth by Taylor resulted in the conclusion that the basic cause of the problem was the positive sense of the dihedral effect (C_{l_β}). What Taylor's analysis did not do was present a physical explanation of the phenomenon.

In an effort to assure that the problem had been interpreted correctly by the authors, the initial theoretical effort was directed toward matching the results of Taylor's investigation. Thus the human transfer function proposed by Taylor was used and a root locus study of the effect of varying pilot gain undertaken.

The set of equations used was as follows:

$$
\begin{array}{lllll}
 & \underline{\beta} & \underline{d\psi} & \underline{\phi} & \underline{\delta_a} \\
(1) & C_{y_\beta} - 2d & -2 & C_L + 2\alpha_o d & 0 \\
 & \mu C_{l_\beta} & C_{l_r}/2 & \frac{C_{l_p}}{2} d - J_x d^2 & \mu C_{l_{\delta_a}} \\
 & \mu C_{n_\beta} & \frac{C_{n_r}}{2} - J_z d & \frac{C_{n_p}}{2} d & \mu C_{n_{\delta_a}} \\
 & 0 & 0 & K(1 + .57d) & -1
\end{array}
$$

It is worthy of note that the above set is for a principal axes coordinate system. This particular coordinate system was chosen for this study inasmuch as the stability derivatives as obtained from Ref. 5 had been calculated with respect to this system of axes.

The result of the root locus study can best be explained by considering separately the effect of varying

the pilot gain, K, and the trim angle of attack, α_0. The fact that α_0 was a significant parameter actually was determined during the analog computer phase of this program and is discussed in detail in connection with that part of the program. Here the fact that α_0 is important will merely be stated and then substantiated by the root locus technique.

Assuming the pilot gain to be the variable of interest, the determinant of the coefficients of (1) was expanded with the following root locus equation resulting:

$$(2) \quad \frac{(\lambda+\lambda_r)(\lambda-\lambda_s)(\lambda^2+2\zeta_\psi\omega_{n\psi}\lambda+\omega_{n\psi}^2)}{(\lambda^2+2\zeta_\phi\omega_{n\phi}\lambda+\omega_{n\phi}^2)(1+.57\lambda)}+\frac{\mu C_{l\delta_a}}{J_x}K=0$$

The derivation of the above equation is included in Appendix B.

Figure 8a was the type of root locus which resulted from the above equation when α_0 was assumed to be negligible. This root locus showed the inclusion of a proportional pilot gain to be a stabilizing factor at zero angle of attack, provided the stability derivatives could be assumed constant. Furthermore, a study of the parameters which determine the value of $\omega_{n\phi}$, (Eq. 5 in Appendix B), reveals that an increase in either of the two suspect stability derivatives ($C_{n\delta_a}$ and $C_{l\beta}$) would actually decrease the value of $\omega_{n\phi}$ and thus tend to stabilize the closed loop system. This is a result of the signs of both derivatives being reversed from what might be termed normal.

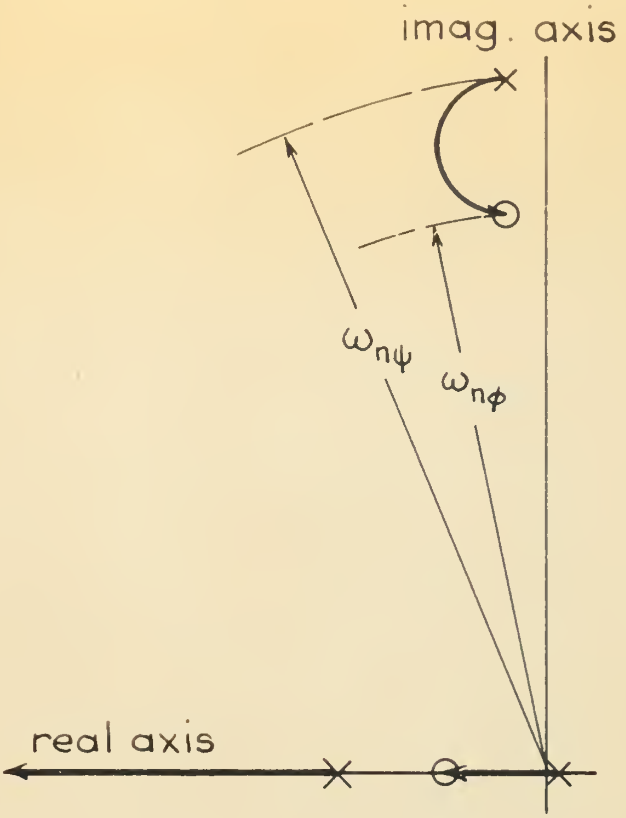

Fig. 8a. Root Locus for $\alpha_0 = 0$, $0 < K < \infty$

The next step was to include the correct value of α_0 (10 degrees). From equations (1) it can be seen that the inclusion of α_0 has no effect upon the denominator term of the root locus equation but does alter the characteristic equation somewhat. The added terms which are the result of including α_0 are:

$$(3) \quad \alpha_0 \left[\frac{\mu}{2 J_x J_z} (C_{l\beta} C_{n_r} - C_{n\beta} C_{l_r}) \lambda - \frac{\mu C_{l\beta}}{J_x} \lambda^2 \right]$$

It can be seen from equation (3) that with a positive $C_{l\beta}$ and all other derivatives of the usual sign, the effect of including α_0 is to decrease the λ and λ^2 terms of the characteristic equation. This had little effect upon the roll and spiral modes but did result in

both the damping ratio (ξ_ψ) and the undamped natural frequency ($\omega_{n\psi}$) of the Dutch roll mode being appreciably decreased. The root locus which resulted is depicted by Fig. 8b.

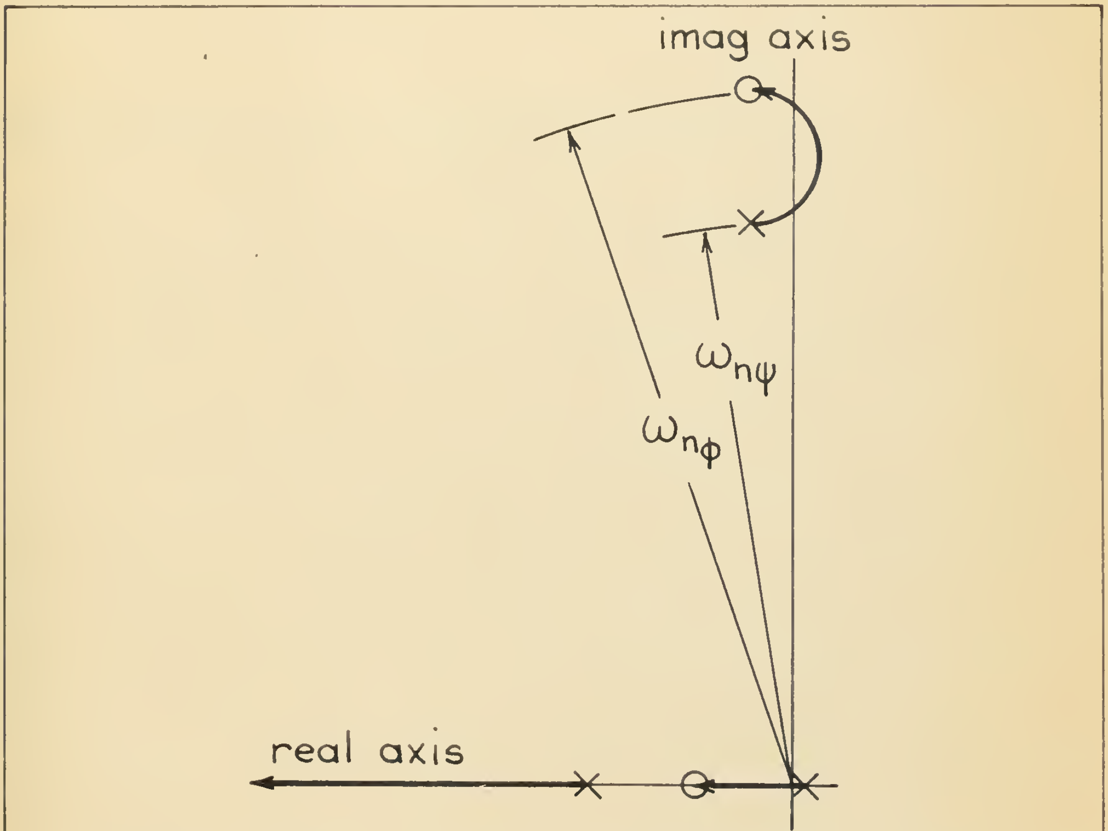

Fig 8b. Root Locus for $\alpha_o = 10°$, $0 < K < \infty$

This is similar to what Taylor obtained. Furthermore, it can be seen from equation (3) that the destabilizing effect of α_o can be attributed to the positive sign of the dihedral effect. (C_{l_β}).

Having shown the importance of the trim angle of attack, it was deduced that a root locus using trim angle of attack (α_o) as the varying quantity might be informative. This study was carried out by assuming the

stability derivatives to be independent of the trim angle of attack. Thus only the orientation of the aircraft with respect to its flight path was assumed to be variable. The root locus equation for this investigation had the following form:

$$(4)\quad \frac{(\lambda+\lambda_r)(\lambda+\lambda_s)(\lambda^2+2\zeta_\psi\omega_{n\psi}+\omega_{n\psi}^2)}{\lambda(\lambda+K''/K')} + K'\alpha_o = 0$$

with the denominator terms found from equation (3) and with $K' = -\mu C_{l\beta}/J_x$ and $K'' = \frac{\mu}{2J_xJ_z}(C_{l\beta}C_{n_r} - C_{n_p}C_{l_r})$

Figure 8c shows the root locus for $0 \leq \alpha_o \leq \infty$ for no pilot gain while figure 8d shows the same result for an arbitrary pilot gain. Calculations for the conditions investigated showed the system with pilot gain to go unstable for a trim angle of attack on the order of twenty five percent of what was required for instability without the pilot in the loop. Conversely it was noted that for a trim angle of attack of ten degrees, the open loop system was so slightly stable that a small pilot gain could be expected to be sufficient to cause the closed loop instability. From equation (4) it can be seen that a negative $C_{l\beta}$ would change the sign of K' and in turn change the angle condition for the root locus diagram. For this case, the effect of increasing α_o would not be destabilizing.

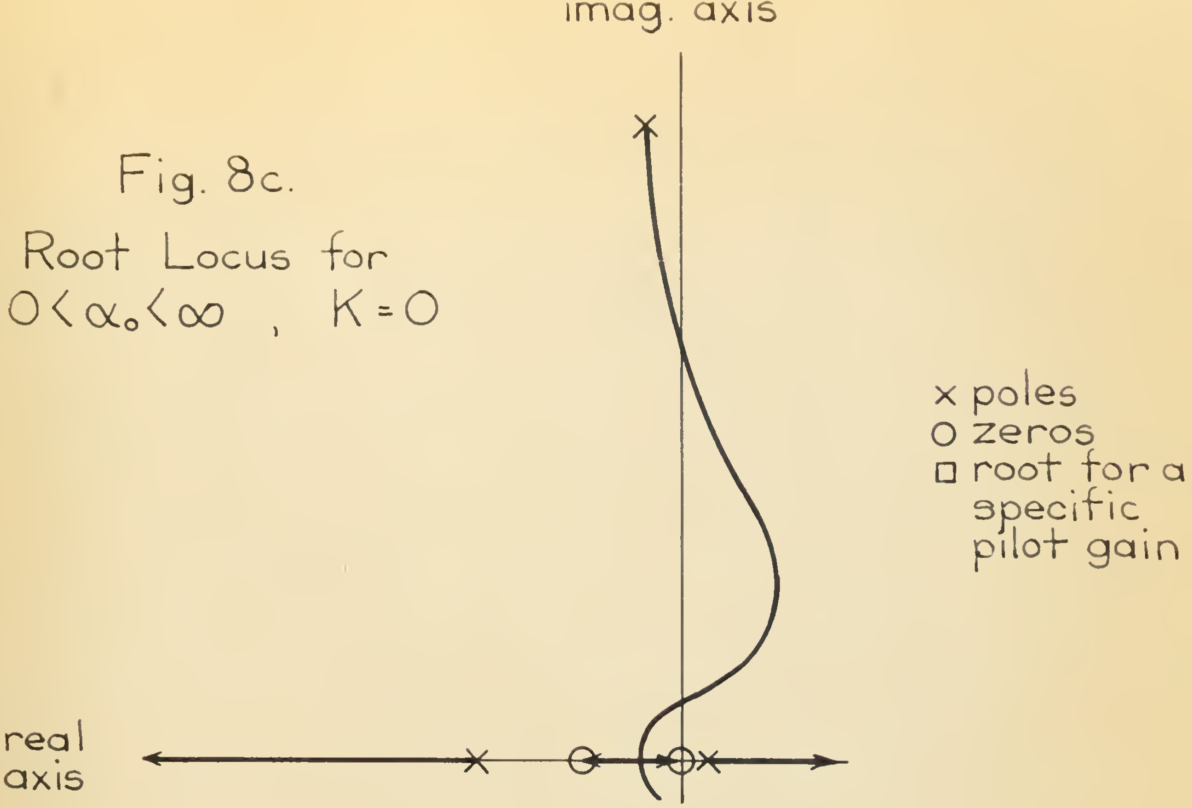

Fig. 8c.

Root Locus for $0<\alpha_0<\infty$, $K=0$

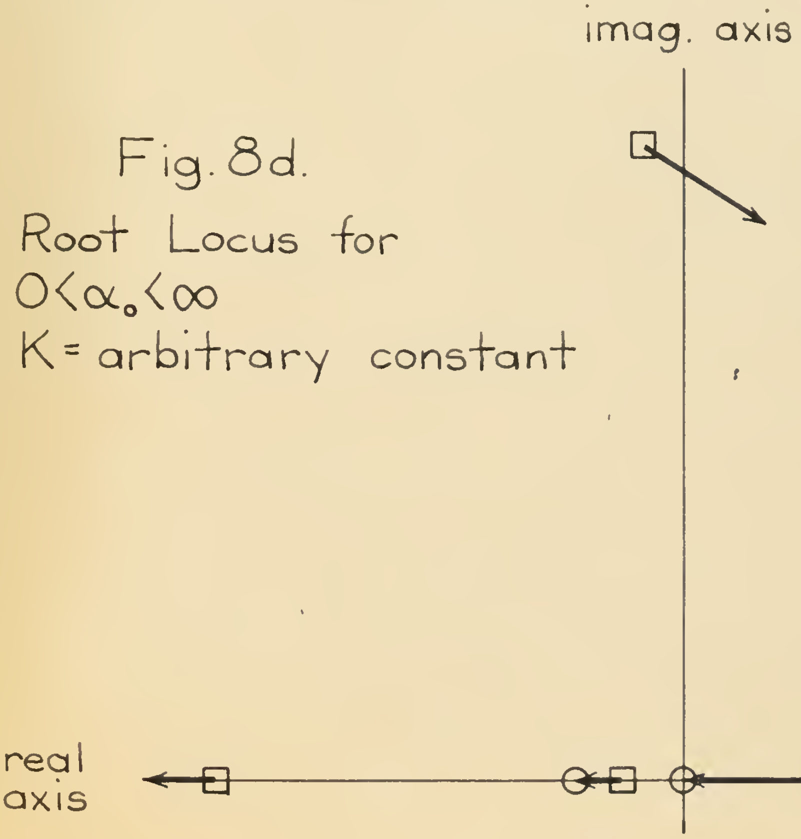

Fig. 8d.

Root Locus for
$0<\alpha_0<\infty$
K = arbitrary constant

Several interesting observations resulted from a study of the root loci briefly discussed above. First, it was observed that if the signs of both the dihedral effect (C_{l_β}) and the aileron yaw ($C_{n_{\delta_a}}$) had been reversed, there would have been virtually no change in the closed loop response at low angles of attack. However, a study of the cofactor of the (α_0) term showed that a beneficial effect would have been realized as the trim angle was increased. Secondly, the observation was made that for a positive dihedral effect, the proverse sense of the aileron yaw definitely tended to improve the closed loop stability while an adverse aileron yaw would have had the opposite effect. That is, an adverse aileron yaw would have placed the complex zero (Fig. 8b) even further above the complex pole. This was believed to be particularly significant inasmuch as with pilot time lag removed as a significant contributor to the instability, one might reason that the only way that the pilot could be contributory as a destabilizing factor would be as a means for introducing an unfavorable forcing function while actually responding correctly to the error signal. In the case of a single control, this meant an unfavorable input into either the rolling or yawing moment equations by means of an aileron deflection. For the particular case investigated, the root locus plots showed a proverse aileron yaw ($C_{n_{\delta_a}}$)

to be favorable while an increase in the trim angle (α_o) was seen to have a destabilizing effect. Thus it was reasoned that the probable physical effect was that an increase in trim angle of attack opposed the proverse aileron yaw effect until, at some angle of attack, the sense of the sideslip resultant from an aileron deflection was probably reversed. This might be explained by noting that a simple uncoupled rolling motion about the body axis of an aircraft will result, as the roll angle increases, in the conversion of angle of attack into sideslip angle. For example, a positive roll would tend to produce a positive sideslip. This is the opposite of the effect produced by a proverse aileron yaw. Thus it is reasonable to assume that at some point the effect of angle of attack and of proverse aileron yaw might be equal. At this point and beyond, an increase in the pilot gain would cause the pilot to introduce a destabilizing force. Looked at in the light of Taylor's analysis, this point where the aileron yawing moment due to aileron deflection reversed direction is probably coincident with the point where ω_ϕ/ω_ψ becomes greater than unity.

In summary, the theoretical effect agreed quite well with Taylor's analysis although it is felt by the authors that the approach involving the variation of trim angle of attack provided a basis for the physical reasoning explained above. However, it can be seen that even if

the physical effect of increasing the trim angle is as stated, the mechanism by which the instability occurs cannot be explained from the theory alone. Fortunately, a study of the time histories of both the analog computer simulator and the variable stability NAvion did provide an insight into the mechanism involved and did tend to agree with the hypothesis suggested by the theory.

Analog Computer - Simulator Phase:

As mentioned previously, the approach used in this investigation was to make a detailed study of an airplane-pilot combination which results had shown to be unstable. For the computer phase of the investigation two variations, along with the basic condition, were examined. The basic condition was the X-15 research airplane flying at M = 3.0 with an angle of attack of ten degrees. The two variations were: to keep all other conditions the same but decrease the trim angle of attack to zero, and to keep all other conditions the same while increasing the dynamic pressure from 153 to 1,000 pounds per square foot. All three of these conditions will be discussed below.

Condition I: $M = 3.0$, $q = 153\#/ft^2$, $\alpha_o = 0$

For this condition, the basic equations of motion, using the non-dimensional X-15 coefficients, reduce to the following set of computer equations:

$$100\dot{\beta} = -3.35\beta - 100\dot{\psi} + 1.067\phi$$
$$.2\ddot{\phi} = 1.67\beta + .0345\dot{\psi} - .042\dot{\phi} + 3.66\delta_a$$
$$10\ddot{\psi} = 60\beta - .451\dot{\psi} - .0451\dot{\phi} + 9.9\delta_a$$

Both step aileron inputs and "attempts-to-fly" the computer simulator showed this condition to be completely manageable without the slightest tendency to go unstable.

This fact, in conjunction with the other studies outlined herein, confirmed the significance of the trim angle of attack (α_o) to the study of the closed loop instability.

Condition II: $M = 3.0$, $q = 153\#/ft^2$, $\alpha_o = 10$ degrees

This condition resulted from an analysis of the results of Condition I. By re-evaluation of the basic equations, using $\alpha_o = 10$ degrees, the following set of equations was obtained:

$$100\dot{\beta} = -3.35\beta - 100\dot{\psi} + 1.067\phi + 17.45\dot{\phi}$$
$$10\ddot{\phi} = 90\beta + 1.725\dot{\psi} - 2.12\dot{\phi} + 83.9\delta_a$$
$$20\ddot{\psi} = 55\beta - .902\dot{\psi} - .0902\dot{\phi} + 9.08\delta_a$$

These equations were mechanized into the computer and resulted in the predicted pilot-induced instability.

A step aileron input and an "attempt-to-fly" the computer are shown in Figures 9 and 10. From the step

FIG. 9
COMPUTER RESPONSE TO STEP AILERON INPUT ; $q = 1000$ psf
$\alpha_o = +10°$ $M = 3.0$

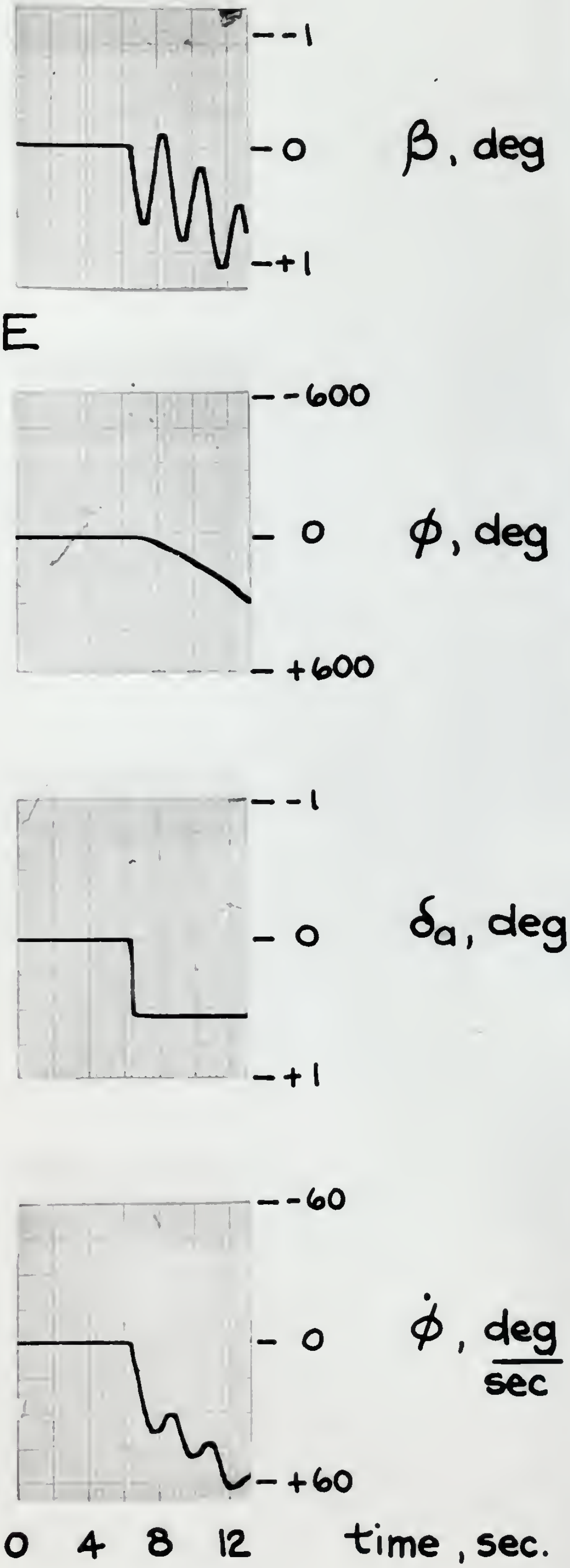

FIG. 10

ATTEMPT
TO FLY
SIMULATOR

$q = 1000$ psf
$\alpha_0 = 10°$
$M = 3.0$

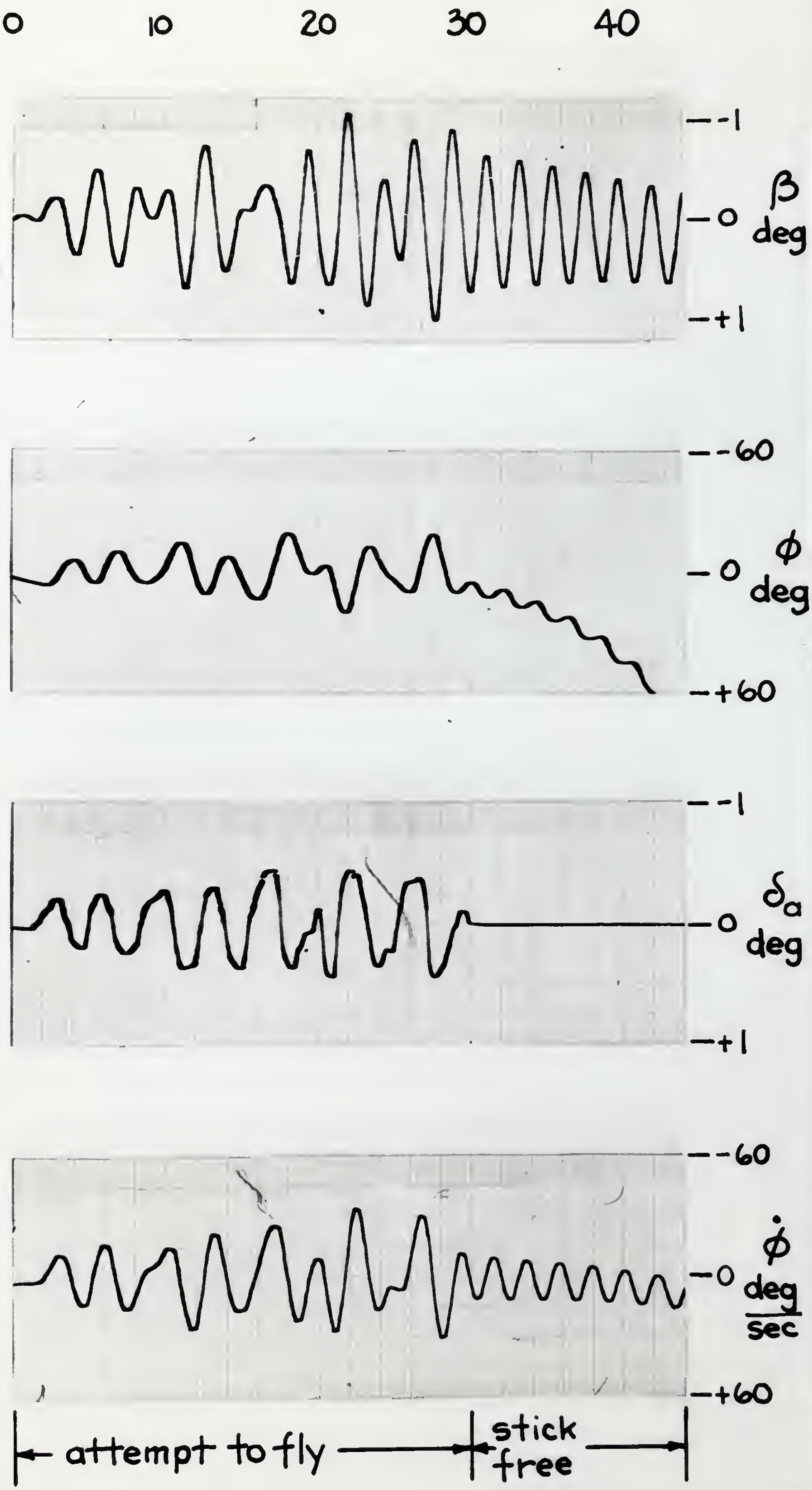

input response there were several important things noted. First, it was seen that the motion was lightly damped. Second, there was considerable excitation of the Dutch roll mode from a coupling of the rolling and yawing modes of motion. Third, although the sign of $C_{n_{\delta_a}}$ was positive - leading one to believe the yaw, and consequently the sideslip, due to aileron should have been proverse - the total effect of the parameters affecting the sideslip was just the opposite. That is, the sideslip angle response described by these equations, due to a step aileron input, was as might be expected from an adverse yawing moment. The fourth and last item to be noted was the phase angle difference between the angle of roll and the angle of sideslip. It could be seen from the time histories, that the two motions were almost exactly out of phase. The significance of the phasing of these angles while the Dutch roll motion was in progress, as well as the sign of the sideslip resulting from an aileron input, will be discussed more fully later.

Using the control stick simulator, "attempts-to-fly" the simulator resulted in oscillations of increasing amplitude if the "pilot" responded in a normal manner to bank angle and roll rate. Using the stick to make aileron inputs in an effort to keep the wings level resulted in an increase of the sideslip angle , due to the aileron deflection. Thus, sideslip grew, fed the

roll excursions, and the resultant situation was one of a closed loop instability. By releasing the stick, the oscillations damped out, although the roll angle grew indefinitely as a result of the unstable spiral mode.

An "attempt-to-fly" the computer by using the $\dot{\beta}$ technique described by Petersen in Reference 6 was completely successful. The oscillations were allowed to build up using normal pilot techniques, and then, at some point, ailerons were used primarily to stop the sideslipping, and secondarily to keep the wings level. As the β trace came through zero, the stick controller would give the stick a sharp pulse in the direction the trace was moving. In the airplane this would correspond to a sharp right aileron pulse as the nose of the airplane went through zero degrees sideslip heading toward the right. In this manner, the motion could be damped out within a few cycles. It did not appear feasible to maintain steady state conditions using this technique, but oscillations resulting from normal pilot inputs could be rapidly damped out in this manner. Roll angle control was maintained by varying the magnitude of the pulse and the stick position between pulses.

During the study of this condition, the following observations were noted:

1. The oscillatory motion was lightly damped,
2. There was considerable coupling between the roll and sideslip motions,

3. The sideslip generated by an aileron deflection was adverse even though $C_{n\delta_a}$ was positive.
4. During Dutch roll oscillations the angles of bank and sideslip remained approximately 180 degrees out of phase.
5. Normal attempts-to-fly were unsuccessful, and
6. The $\dot{\beta}$ technique could be used to damp out any Dutch roll oscillations that developed.

Condition III: $M = 3.0$, $q = 1000\#/ft^2$, $\alpha_0 = 10$ degrees

This condition was investigated primarily to see if the characteristics of the motion were affected by changes in dynamic pressure. The basic equations of motion modified to increase the dynamic pressure were written as:

$$20\dot{\beta} = -4.52\beta - 20\dot{\psi} + 1.44\phi + 3.49\dot{\phi}$$
$$2\ddot{\phi} = 116.8\beta + 2.32\dot{\psi} - 2.84\dot{\phi} + 108.4\delta_a$$
$$4\ddot{\psi} = 71.2\beta - 1.212\dot{\psi} - .1212\dot{\phi} + 11.72\delta_a$$

These equations were mechanized in the computer and both step aileron inputs and "attempts-to-fly" were observed. The basic character of the motion did not change. All the comments recorded under Condition II are valid for the higher dynamic pressure. The only significant change in the motion was the frequency of oscillation of the Dutch roll mode. Previously the motion had a period of about five seconds. At this increased dynamic pressure the period was reduced to

approximately two seconds. This did not alter the difficulty of attempting to fly the configuration. Nor did the increased frequency invalidate the $\dot{\beta}$ technique of control.

This condition can be summed up simply by saying it was identical to Condition II except things happened a little faster. However, the motion was not so fast as to make the controller's task too difficult, nor so fast that the character of the motion and subsequent responses to the motion were changed.

One result of the above observations was that the frequency of the motion (within the limits investigated) was seen to be an insignificant contributor to the instability. As long as the motion proceeded at a pace which the controller could follow, and as long as the normal control motions were made, the basic instability occurred. Thus the frequency of the motion was eliminated as an important parameter insofar as a study of the basic destabilizing mechanism was concerned. This confirmed the hypothesis outlined in the theoretical portion of the discussion.

Flight Phase:

The flight phase of this investigation involved the use of the variable stability NAvion. The physical characteristics of this airplane, its simulation equip-

ment and the accompanying instrumentation are described elsewhere in this report.

The initial flight phase was based upon an instability encountered by the X-15 research aircraft in a steady flight (lift = weight) condition at Mach 3 and at ten degrees angle of attack. The dimensional X-15 derivatives used in calculating the potentiometer settings are listed in Table III. A direct method for simulating the X-15 side force equation was not available, and the dynamics introduced by the autopilot equipment were not known by the authors, hence it was necessary to correct the computed autopilot potentiometer gain settings in flight until a desired condition was achieved.

Flight simulation was directed toward achieving the desired character of pilot induced instability, rather than toward an exact simulation of the dynamic response of the X-15. On this premise, and on the basis of computer studies, it was decided that the most significant characteristics to be simulated were the following: 1) a lightly damped Dutch roll mode 2) a roll rate response to an aileron function which contained a significant Dutch roll effect.

Cockpit potentiometer settings were adjusted until the two above characteristics were obtained. It was found that the period of the Dutch roll mode obtained in this manner was approximately three seconds, and the

steady state roll rate of the aircraft was slightly decreased. Thus Dutch roll period is of the same order of magnitude as the periods of the Dutch roll modes studied on the computer. In addition, computer studies indicated that the frequency of the Dutch roll mode was unimportant insofar as the fundamental problem was concerned.

Undoubtedly the most important characteristic was simulated, namely, the closed-loop pilot-airplane system exhibited an unstable Dutch roll oscillation in spite of the fact that the open loop response was lightly damped. Thus, as in the case of the X-15, the attempts of a pilot to improve upon a marginal condition had a destabilizing effect. Significantly, this unstable result could be avoided if the pilot used both ailerons and rudder for control. Just why the authors feel this point to be significant will be discussed later in this report.

Time histories of the various angles and rates as recorded on a typical flight are included herein. Inasmuch as the mode of interest was the Dutch roll, the authors felt the two most significant time histories to be those of the sideslip angle (β) and the roll rate ($\dot{\phi}$). Accordingly, the time histories of these two items were studied in detail and will be the items discussed herein.

It can be seen from the time histories of the airplane response to a step aileron input (Fig. 11), that the roll rate did contain a considerable amount of Dutch roll, and further, that the Dutch roll motion was lightly damped. Also, it can be seen that the proverse sense of the aileron yaw resulted in the initial sideslip generated by an aileron input being of opposite sign to the roll rate response. This was as might be expected for an airplane with appreciable proverse aileron yaw and only a slight amount of yaw due to roll. However, this initial sideslip response to an aileron input was the opposite of what was observed to happen on the analog computer simulator. With the benefit of hindsight, it can be stated that this difference was probably due to the fact that the effect of the trim angle of attack (α_0) had not been considered.

From the time histories of the attempts to fly the resultant configuration, (Fig. 12) it can be seen that attempts by the pilot to control the oscillation resulted in excursions of increasing magnitude for both the sideslip angle and the roll rate. Releasing the controls, (Fig. 13) on the other hand, resulted in decreasing amplitudes of motion. However, once large amplitudes of motion had been obtained, what appeared to be a limit cycling of the autopilot prevented a complete damping of the open loop motion. An important piece of information

FIG. 11
RESPONSE TO STEP AILERON INPUT

Navion Variable Stability Aircraft

Basic X-15 Settings

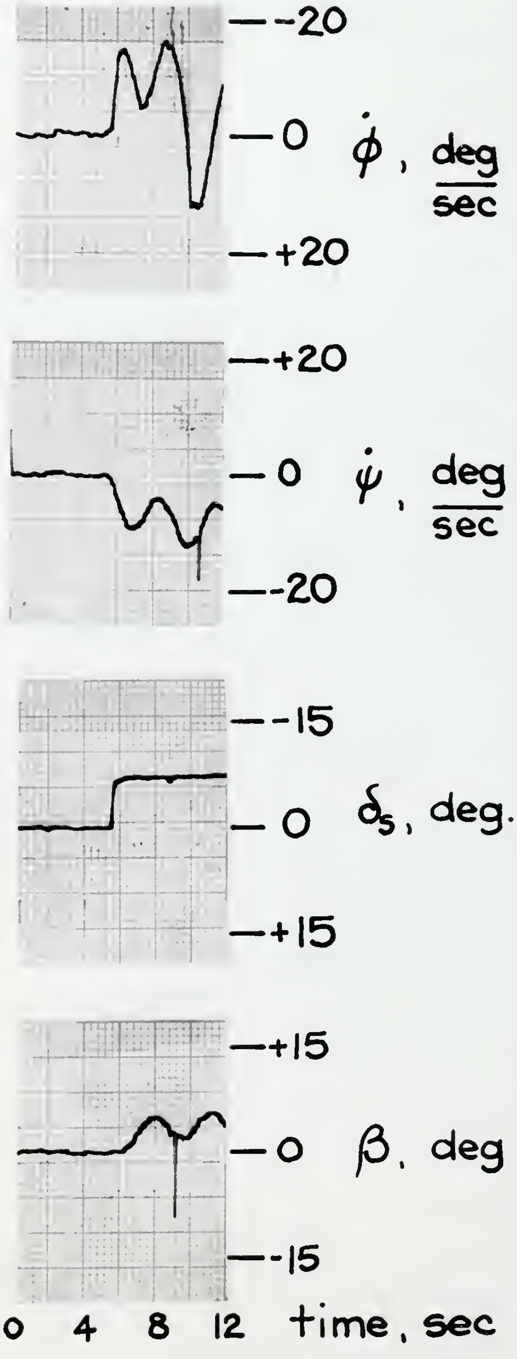

FIG. 12
PILOT-INDUCED INSTABILITY
Navion Variable Stability Aircraft

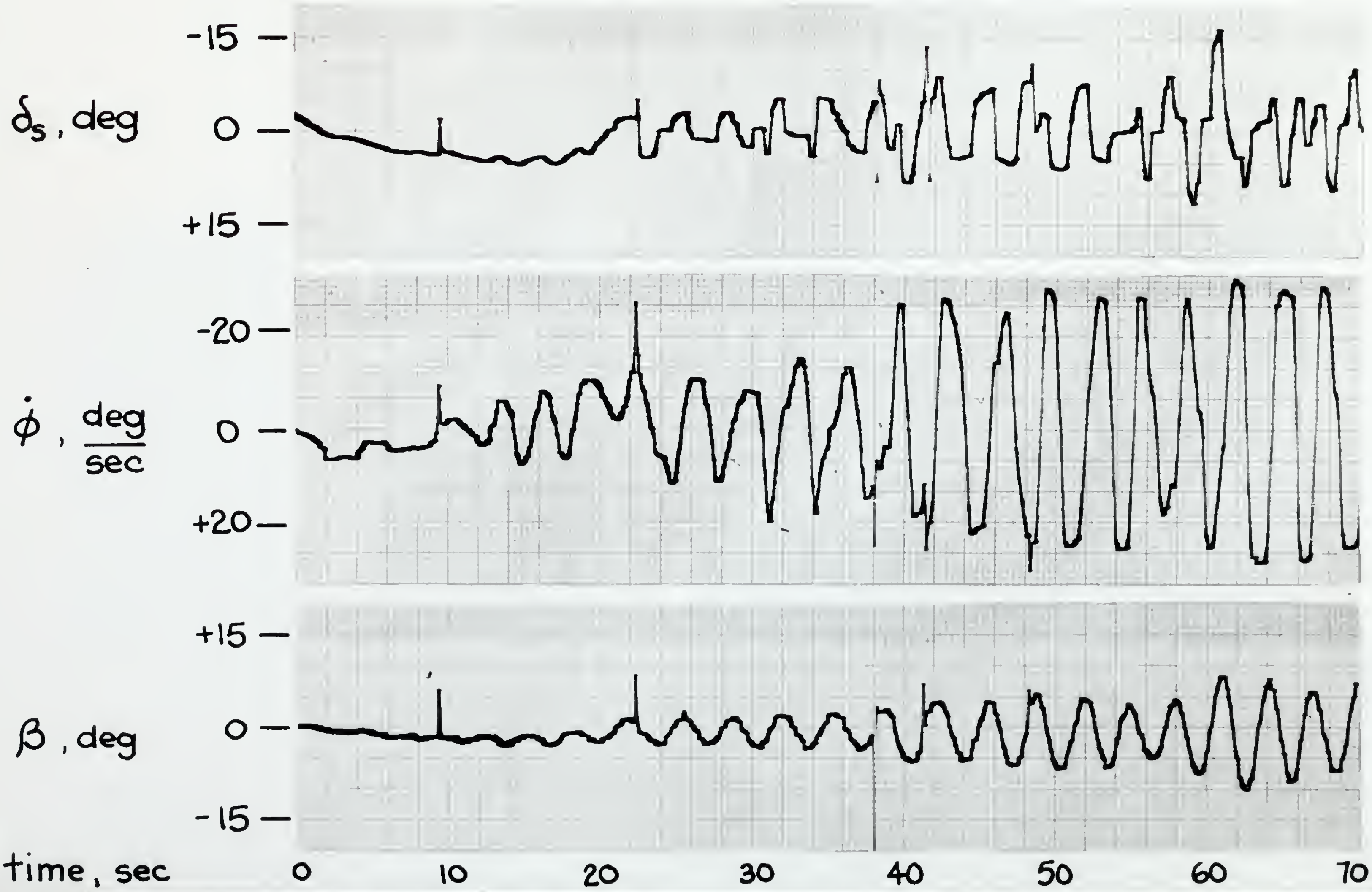

FIG. 13
OPEN LOOP
DUTCH ROLL
CONVERGENCE

Navion Variable
Stability Aircraft

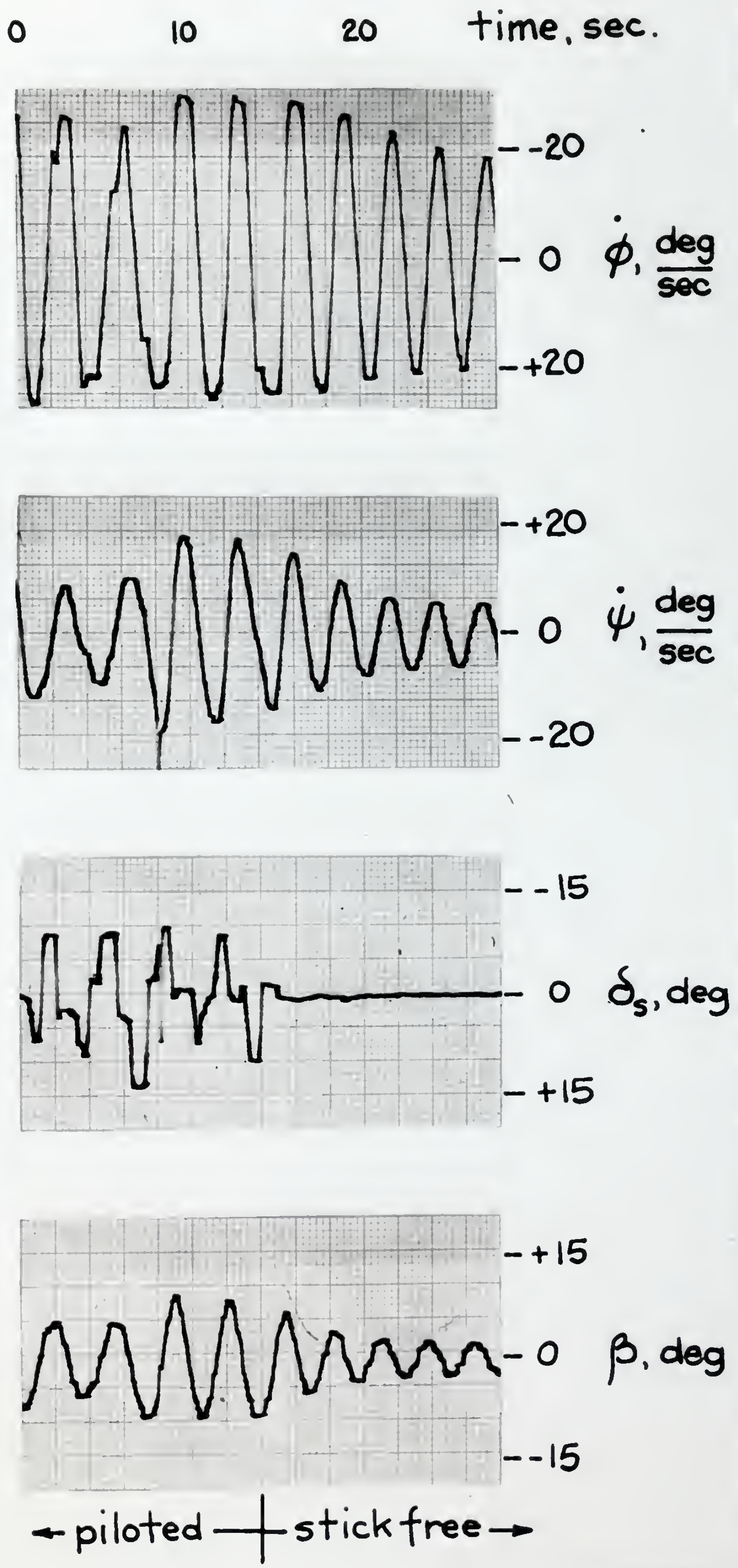

that can be obtained from these time histories is the phase relationship of the sideslip angle (β) and the roll angle (ϕ) - the latter being assumed to lag the roll rate by a quarter of a cycle. In particular, it can be seen that the sideslip angle and the roll angle are almost exactly in phase. This was also in contrast to the phasing obtained by the electronic analog simulator. Thus it was noted that both the analog simulator and the NAvion simulator exhibited a pilot induced oscillation in spite of the fact that the character of the motion was virtually opposite for the two cases. That the sideslip resulting from a step aileron input was also different for the two systems suggested the possibility that, in spite of the apparent difference, the same destabilizing mechanism was involved in each case. Accordingly, the aileron yaw was reversed from the proverse to the adverse sense and the tests repeated. Time histories (Fig. 14) show that although the response of sideslip angle to an aileron input was reversed, the percent of Dutch roll in roll was maintained at a high level and the Dutch roll remained lightly damped. However, this configuration could be controlled by the pilot. This is not to say that the resultant configuration was a good - or even acceptable - airplane from a handling qualities standpoint. The damping of the Dutch roll mode was so slight that unpleasant oscillations developed rather easily - particularly if rapid control reversals were attempted.

FIG. 14

RESPONSE TO STEP AILERON INPUT

Navion Variable Stability Aircraft

Adverse Aileron Yaw

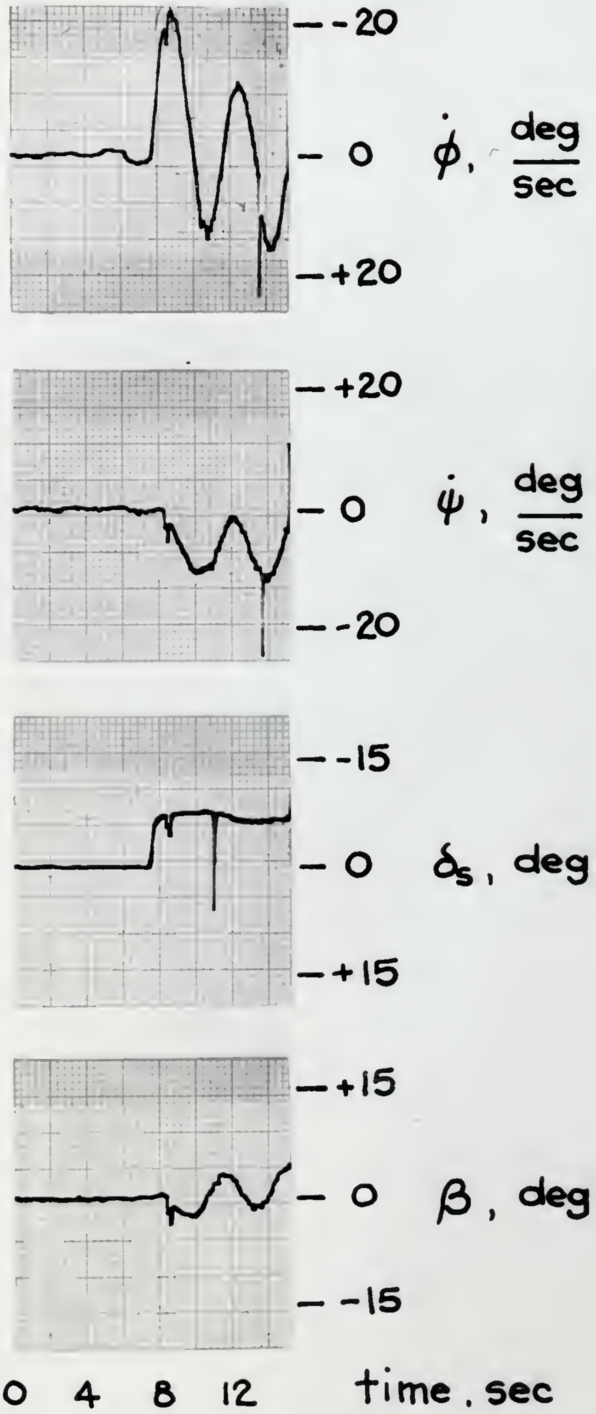

However, it is significant that the pilot was able to control the aircraft, and, in fact, damp the oscillations when they occurred using only normal aileron control movements. This seemed to confirm the hypothesis that the destabilizing mechanism for the X-15 pilot-aircraft combination (as manifested by the analog simulator) was of a similar character to what was obtained with the NAvion. In particular, it could be seen that the instability resulted when the pilot, in an attempt to control roll angle, succeeded in reducing the roll angle only at the expense of increasing the sideslip angle.

During this flight phase, flight of the basic (closed loop unstable) configuration using both ailerons and the rudder to maintain lateral-directional control was tried. The results showed that by using the rudder, the sideslip angle could be controlled and the aircraft handled comparatively easily. Rapid reversals presented a problem as it was difficult to keep the aircraft in balanced flight throughout the maneuver and a rather large Dutch roll oscillation often resulted. However, by using rudders, the oscillations could be damped within a few cycles, (Fig. 15). This also tended to confirm the importance of the sideslip angle to the oscillation.

Aerodynamic derivatives other than the aileron yaw were varied and a pilot opinion of these variations obtained. However, even though many of these derivatives

FIG. 15

BOTH AILERONS AND RUDDERS USED

Navion Variable Stability Aircraft

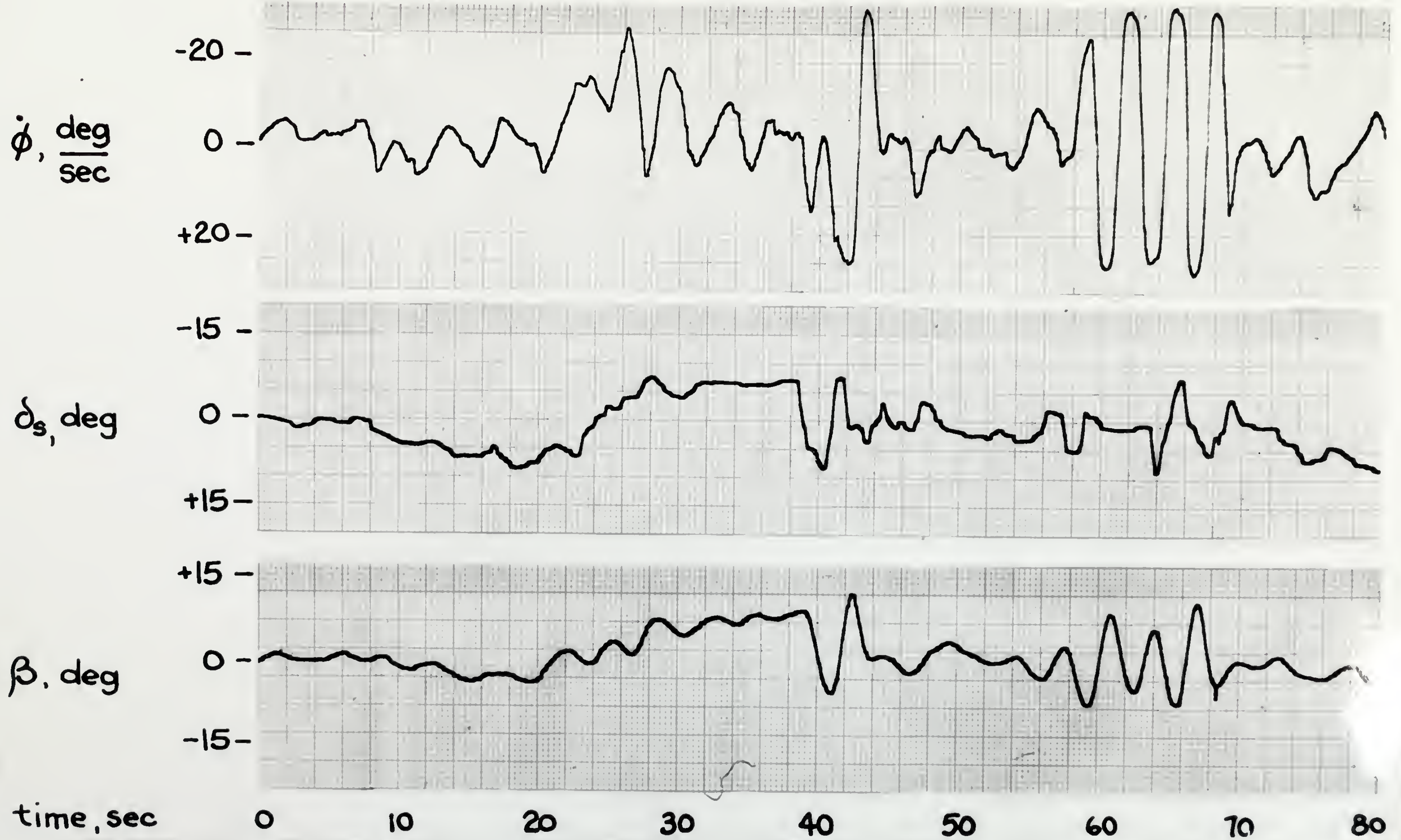

were found to have an important effect upon the handling qualities, none were found to be so directly involved in the actual destabilizing action of the pilot as the aileron yaw, but rather were indirect contributions to the problem. As such, the effects of these other stability derivatives were probably of importance in establishing the conditions believed to be necessary for a problem of this type to exist. These conditions are further discussed in the following section.

The reason for the difference in phasing of roll and sideslip between the computer and NAvion is believed to lie in the inability to directly simulate the side force equation with the NAvion. An attempt was made to adjust the NAvion stability derivatives in such a way as to allow for the effect of trim angle of attack (α_0). Flight test of this altered configuration, however, indicated that the phasing had not been changed.

The fact that the NAvion did not yield the same phasing of sideslip and roll as was obtained with the analog computer was not considered by the authors to be a shortcoming of the flight simulation. It was felt, rather, that this difference in phasing helped to emphasize the more general nature of the physical explanation of the instability mechanism proposed herein - that is, since the same character of pilot induced

instability was manifested in both of the two different types of systems investigated, the problem is not limited to one particular aircraft. Furthermore, since the analysis of the mechanism of instability is consistent with both of the two types of motion phasing, the applications of the analysis also become less limited.

Summary of Results:

Quite obviously the different phases of this program have resulted in a multi-sided approach to the basic problem of a pilot-induced Dutch roll instability. In general, it can be stated that each phase of the investigation contributed something unique. Thus, in this section of the report, these separate and distinct contributions will be summarized in an effort to show how each contributed toward the formulation of what is believed to be a correct physical explanation of the destabilizing phenomenon.

From the root locus investigations discussed previously, it was determined that, with a positive dihedral effect, an increase in the trim angle of attack (α_0) had a destabilizing effect upon the characteristic open loop response of the X-15. Further, a study of the equations of motion showed that the effect of increasing the trim angle of attack was to increase the coupling of the sideslipping and rolling motions of the aircraft.

In addition, a study of the co-factor of the trim angle of attack (α_o) term, in conjunction with the root locus shown in Figure 8c, indicated that the phasing of the motions was of such a nature that destabilizing moments were generated. Even more significantly, the root locus analysis showed that, under certain conditions, the normal inputs of a pilot attempting to keep the wings level had a destabilizing effect upon the Dutch roll mode. It was then reasoned that inasmuch as pilot response time had not been considered in the analysis, the destabilizing effect of the human controller could not have been the result of erroneously applied corrections to unwanted deviations in roll angle, but rather had to be due to the indirect effects of the resultant aileron deflections. This indirect effect was seen to be the conversion of angle of attack into sideslip. Thus it was concluded that the attempt of a pilot to control roll angle resulted in the generation of a sideslip angle. Further, the phasing between the rolling and sideslipping motions was of such a nature that one motion tended to reinforce the other.

The results obtained as a consequence of the analog computer-simulator phase of this program complemented the theoretical investigation and, in addition, provided an explanation of the actual destabilizing mechanism. The computer studies confirmed the importance of the trim angle of attack to the oscillatory behavior of the system.

Subsequently the root locus investigation was undertaken and the results discussed above obtained.

Study of the time histories obtained during the computer phase of the investigation showed that the Dutch roll oscillation, for the equations representative of the X-15, was characterized by angles of roll and sideslip which were of opposite sign. Further, the open loop response to a step aileron input showed that an input producing a positive roll resulted in an initial positive sideslip (Fig. 9). This was not what was expected, inasmuch as the aileron yaw was proverse and the yaw due to roll was small. However, as has been previously explained, the conversion of angle of attack into sideslip as the result of a rolling motion could produce an effect of this type.

By combining the two effects noted above - which would be the natural result of a pilot attempting to control a Dutch roll motion with ailerons - it could be seen that an attempt to control the angle of bank in a normal manner would result in an input tending to increase the angle of sideslip. With the high degree of coupling present between sideslip and roll, as evidenced by the considerable Dutch roll contribution to the roll rate time history, an unstable behavior resulted. This hypothesis was checked by artificially increasing the proverse aileron yaw to such an extent that the initial sideslip generated by a step aileron input was changed.

That is, an input which resulted in a positive roll yielded a negative sideslip. Figures 16 and 17 show the time histories resultant from this configuration. With the increased proverse aileron yaw, the configuration could be controlled in spite of the fact that the Dutch roll mode remained lightly damped and the percentage of Dutch roll in roll remained appreciable. The lightly damped Dutch roll mode did result in easily induced oscillations but, unlike the basic configuration, pilot attempts to control roll angle did not destabilize the system. In fact, as might be expected, it was found that attempts to control the roll angle in a normal manner also helped to reduce the excursions of the sideslip angle.

A by-product of the computer study was the confirmation that the frequency of the oscillation was not a significant contributor to the basic instability. Quite obviously, this does not mean that frequency can always be dismissed as insignificant, but only that an instability of the type studied could exist even at frequencies completely within the control limits of a human being. In this phase, it was found that motions with a period as high as five seconds were completely unmanageable as long as a normal pilot technique was used.

The flight phase of this investigation yielded results which essentially complemented those obtained

FIG. 16

COMPUTER RESPONSE TO STEP AILERON INPUT

Effective Proverse Yaw
$q = 1000$ lb./ft.^{2}; $\alpha_0 = +10°$; $M = 3.0$

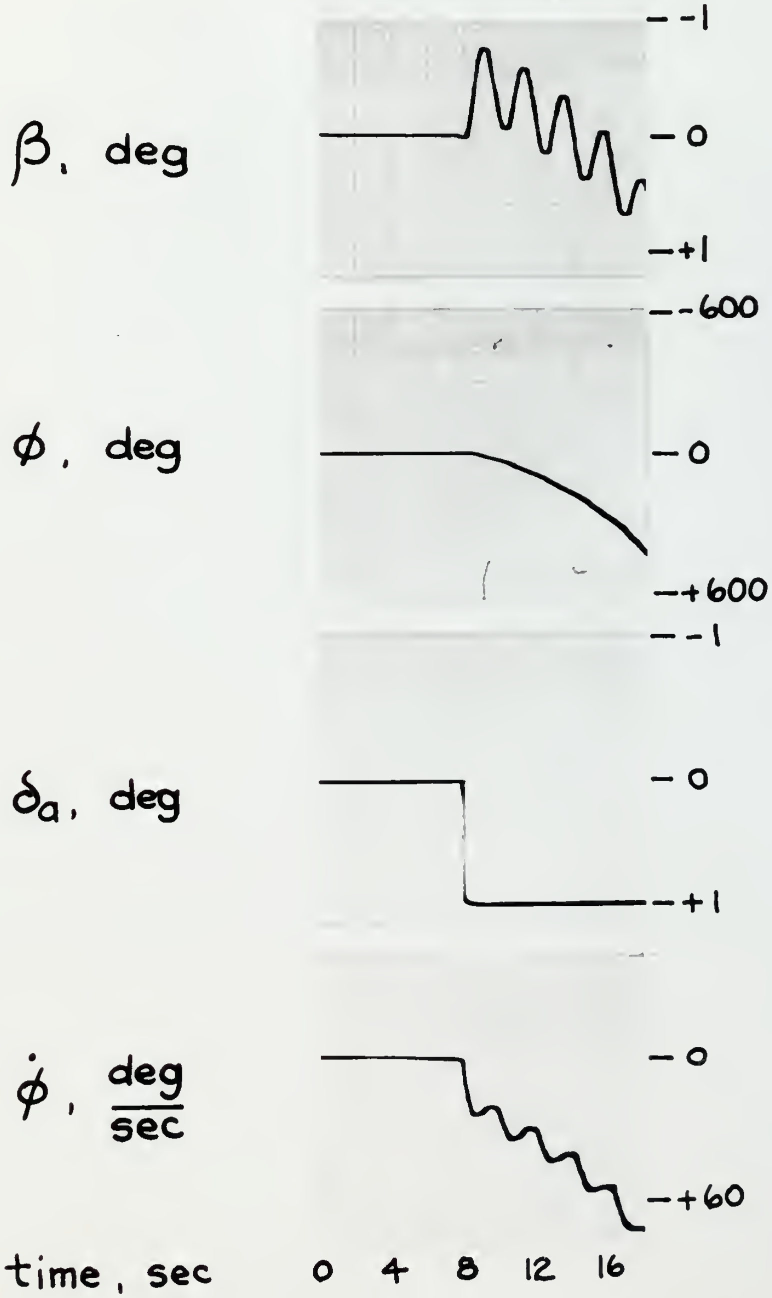

FIG. 17

ATTEMPT TO FLY SIMULATOR - EFFECTIVE PROVERSE YAW

$q = 1000 \text{ lb./ft.}^2 \; ; \; \alpha_o = +10° \; ; \; M = 3.0$

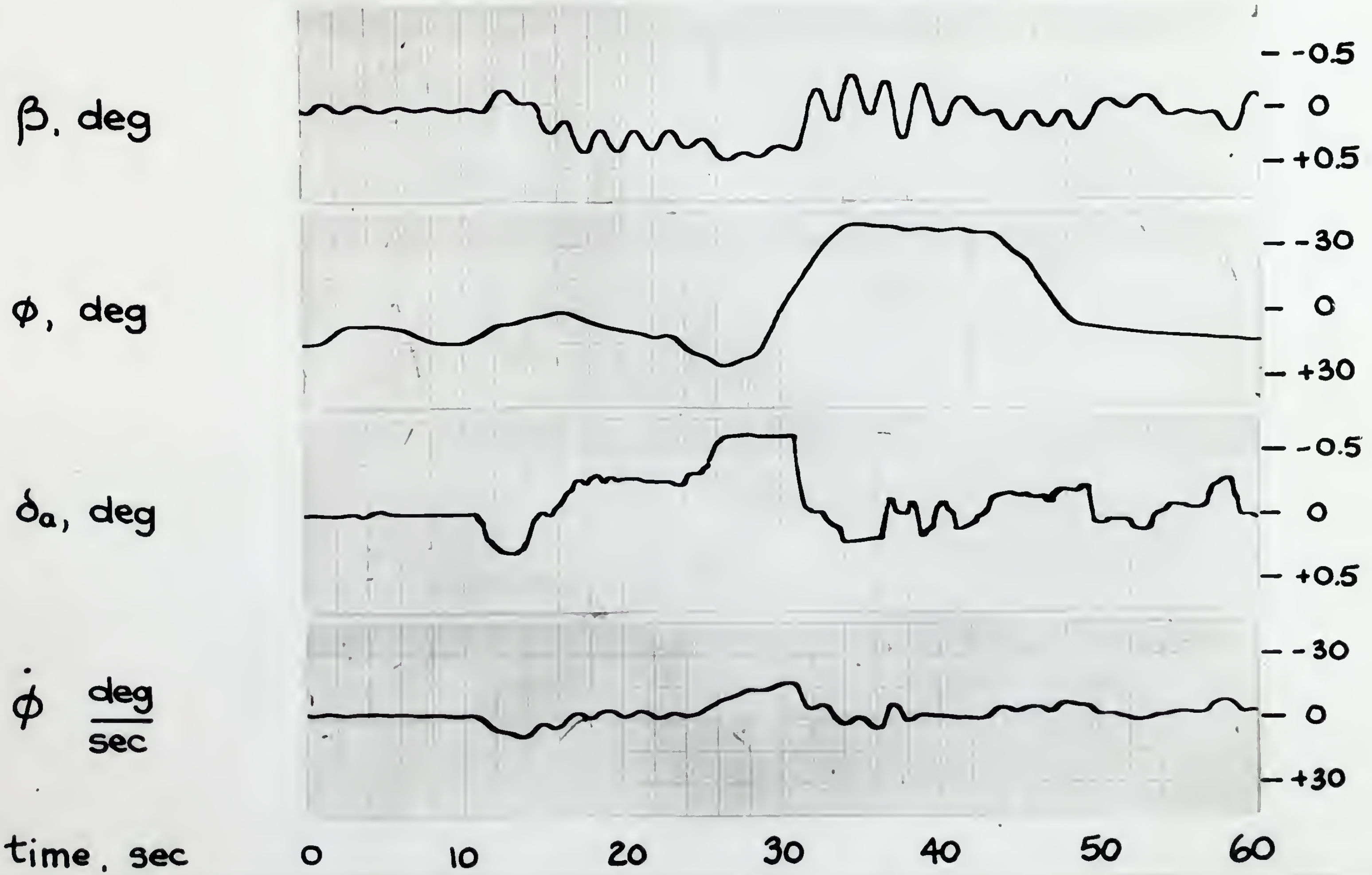

from the fixed base simulator. This was in spite of the fact that the character of the oscillatory motion obtained with the NAvion variable stability airplane was considerably different from what was observed with the fixed base simulator.

As outlined previously, the connection seemed to be that, in either case, an attempt by a pilot to control the roll angle by manipulation of the ailerons resulted in an unfavorable generation of sideslip. Inasmuch as the rolling and sideslipping motions were highly coupled, the increased sideslip generated additional rolling moments which in turn required even greater control movements. The result was a coupled, rolling, sideslipping motion of ever increasing amplitude. That the oscillations could be controlled - or even damped - by judicious use of the rudder, substantiated the validity of the foregoing explanation of the instability mechanism.

The result of the combined studies was that certain combinations of roll angle, sideslip angle, and sideslip resultant from an aileron deflection, were found to be unfavorable. In particular, it was noted that the pilot-induced unstable behavior occurred only when the pilot, in an effort to return to a wings level condition, could not reduce the bank angle without increasing the sideslip angle. Thus an "effective" proverse aileron yaw was found to have a destabilizing

effect if the Dutch roll oscillation was of such a nature that the bank angle and the sideslip angle were in phase. For an "effective" adverse yaw, the opposite phasing was unfavorable. Multiple exposure photographs depicting the two motions described above are included herein. (Figs. 18 and 19). The term "effective" as used refers to the sense of the initial sideslip produced by an aileron deflection. This initial sideslip depends on the combined effects of $C_{n\delta_a}$, C_{n_p} and α_0, rather than the actual sign of the yawing moment produced. Thus it might be termed an integrated effect.

In addition to the above stated phase relationships, certain conditions were necessary before the instability could occur. First, it was necessary that the lateral-directional motions be highly coupled. Physically this was indicated by the large oscillations which occurred in the time histories of roll rate response to a step aileron input. Secondly, it was necessary that the Dutch roll mode be lightly damped. No formal proof of this last statement has been offered herein, but it seems quite obvious that a highly damped mode would virtually never demand pilot attention. Practically speaking, the pilot would probably never be aware of its existence. Accordingly, one could hardly expect the pilot to ever initiate the destabilizing mechanism described above. From a root locus standpoint, an increase in the Dutch roll damping

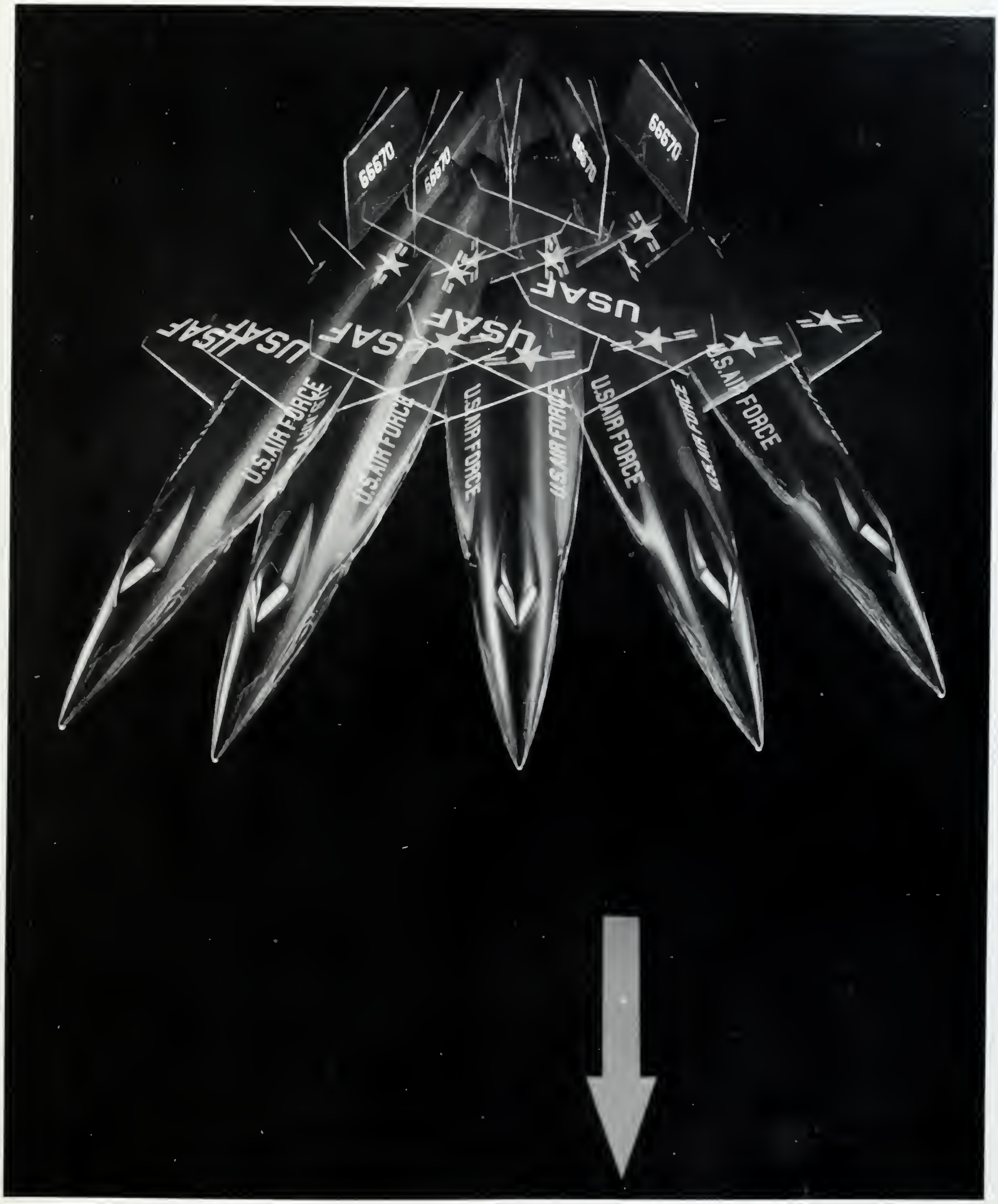

Fig. 18
Dutch Roll Motion
β and ϕ of Opposite Phase

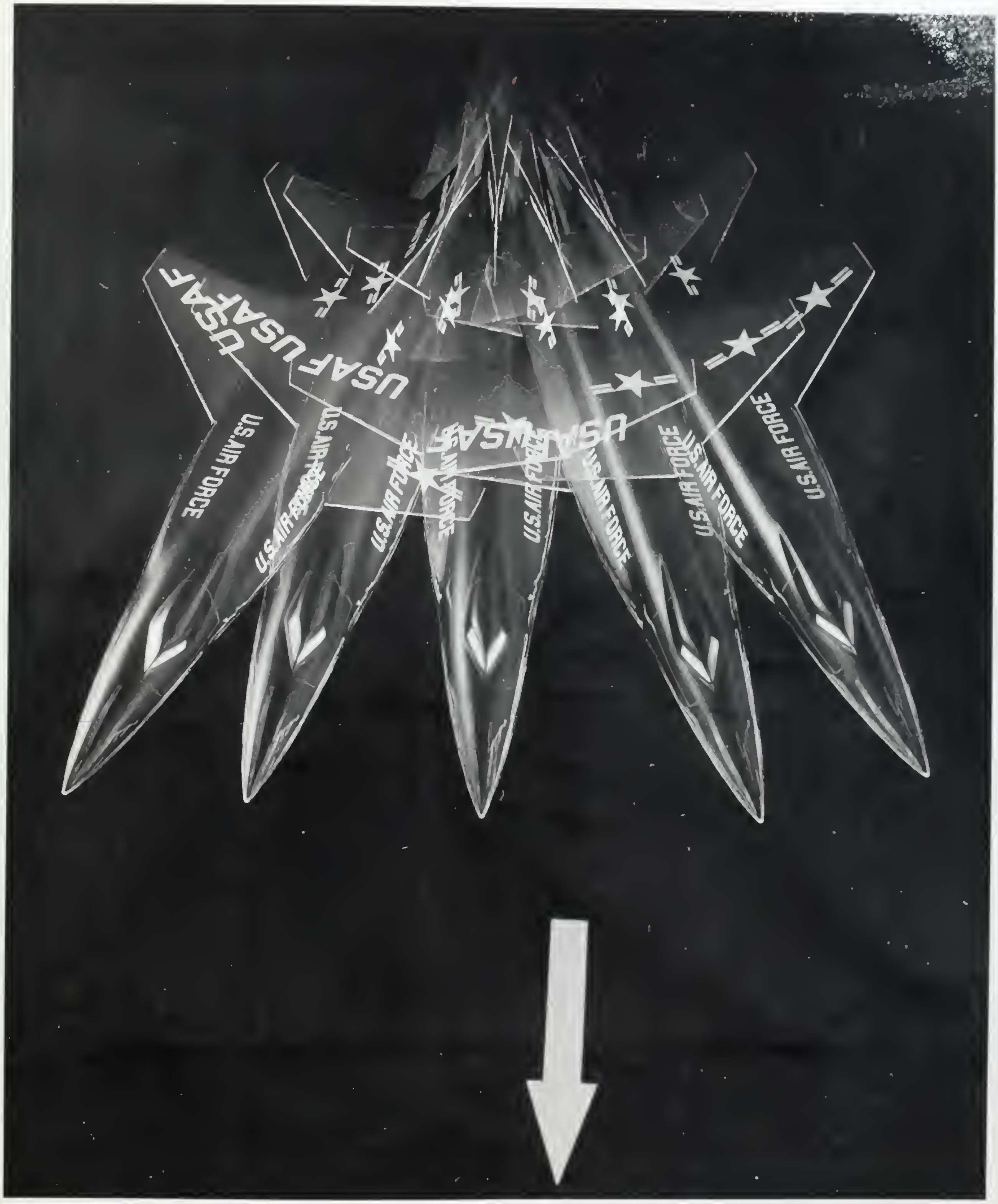

Fig. 19

Dutch Roll Motion

β and ϕ of the Same Phase

would shift the Dutch roll poles and zeroes (Figs. 8a and 8b) to the left. This would obviously have a stabilizing effect.

From the discussion of the destabilizing mechanism, it is apparent that the phasing between the bank angle (ϕ) and the sideslip angle (β) is an important indicator of how a closed loop instability might develop. In particular, this phase relationship determines the sense of the effective aileron yaw that can be regarded as unfavorable. Accordingly, a study was undertaken in an effort to ascertain what parameters determined this phase relationship. This study is outlined in Appendix C. Briefly, the phase angle between ϕ and β was found to be heavily dependent upon the sign of the term: $-2\mu C_{l_\beta}\frac{C_{n_{\delta_a}}}{C_{l_{\delta_a}}}$ This same combination of derivatives has been found to be important in the determination of the ω_ϕ/ω_ψ parameter.

Further analysis led to the conclusion that the phasing of the Dutch roll in roll could be expected to bear some relationship to the character of the roll rate response. Figures 9 and 16 showed that a distinct difference existed between the characteristic time constants of the roll mode for the favorable and unfavorable situations. In particular, the time difference was seen to be approximately equal to one half of the Dutch roll period. This effect is discussed in detail

in Appendix D. Briefly, a shift of 180 degrees (Dutch roll in roll) was seen to coincide with a shift through unity of the magnitude of the $\frac{\omega_\phi}{\omega_\psi}$ parameter.

In summary, for the type of pilot induced instability outlined herein, the arguments presented appear to be a physical way of describing the phenomenon depicted by the root locus studies of Taylor. The theoretical effort conducted in conjunction with this investigation seems to show that the onset of an unfavorable combination of phase relationships is coincident with the parameter described as $\frac{\omega_\phi}{\omega_\psi}$ becoming greater than unity.

Although only a limited number of cases of pilot-induced instabilities were studied in detail in conjunction with this investigation, the authors have seen no reason to suspect that the destabilizing mechanism as outlined herein cannot be regarded in a broader sense. Thus it is the opinion of the authors that an explanation of this type might well be valid for other instabilities known to be a function of pilot gain.

SECTION V

CONCLUSIONS

As a result of this investigation, the following conclusions were drawn:

1. The NAvion variable stability aircraft can be used for a general study of pilot-induced lateral-directional instabilities.
2. A pilot induced instability of the type investigated can be successfully demonstrated, and analyzed with a fixed base simulator incorporating an electronic analog computer.
3. For this type of pilot induced instability of the Dutch roll mode to occur, certain conditions were found to be required. These are listed in a qualitative fashion as:
    a. A lightly damped Dutch roll transient;
    b. Highly coupled rolling and sideslipping motions - as manifested by a large percentage of Dutch roll in roll.
4. If the conditions listed in item (3) were prevalent, certain phase relationships between the roll angle, sideslip angle, and the effective aileron yaw were found to result in an unstable closed-loop system. In particular, if the Dutch roll oscillation showed the roll angle and the sideslip angle to be of the

same sign, an unstable system resulted if the effective aileron yaw was proverse. For the opposite phasing, an effective adverse aileron yaw resulted in an unstable closed loop system.

5. For the type of pilot induced instability studied, the frequency of the oscillation was found to be an unimportant parameter.

6. Even a marginally stable system (open loop) could be managed quite easily if a direct means for controlling the sideslip angle were provided. Accordingly, a system which was closed loop unstable with only aileron control was found to be manageable if the rudder was used. Also, the $\dot{\beta}$ technique could be used, although greater care was required.

7. It was further concluded that this study provided a physical interpretation of the type of pilot-induced instability predictable by the method described by Taylor (Ref. 2).

REFERENCES

1. Ashkenas, Irving L., and McRuer, Duane T., The Determination of Lateral Handling Quality Requirements From Airframe Human Pilot System Studies, WADC, TR 59-135, June 1959.

2. Taylor, Lawrence W., Jr., Analysis of a Pilot-Airplane Lateral Instability Experienced with the X-15 Airplane, NASA TN D-1059, November 1961.

3. Engel, LCDR Gordon R., USN, and Rice, Lt. Daniel W., USN, Influence of Lateral-Directional Responses on Flying Qualities, Princeton University Aeronautical Engineering Department, Rep. 551, May 1961.

4. Ebbert, Lt. E. L., USN, and O'Hara Lt. E. F., USN, A Preliminary Evaluation of the NAvion as a Lateral-Directional Flight Simulator for Use in the Investigation of Flying Qualities Criteria, Princeton University Aeronautical Engineering Department, Rep. No. 509, May 1960.

5. Correspondence from NASA, Edwards Air Force Base.

6. Petersen, Forrest S., Paper presented at Conference on Progress of X-15 Project, November 20, 1961.

TABLE I

PHYSICAL CHARACTERISTICS OF THE NAvion

WING DATA	
Total Area (including ailerons, flaps and 19.87 ft. covered by fuselage)	183.34 ft.^{2}
Span	33.38 ft.
Aspect Ratio	6.05
Taper Ratio	0.54
Dihedral Angle	7.50 deg.
Root Chord	7.20 ft.
Mean Aerodynamic Chord	62.35 in.
Incidence Angle	
Root	2.0 deg.
Tip	-1.0 deg.
Sweepback of Leading Edge	3.0 deg.
Twist	
Geometric	3.0 deg.
Airfoil Section	
Root	NACA 4415R
Tip	NACA 6410R
Flaps, 40 deg., Plain	
AILERON DATA (For one aileron)	
Area	2.16 ft.^{2}
Span	61.99 in.
Deflection	30 deg. up; 20 deg. dwn.

TABLE I (continued)

AILERON DATA (continued)

Control	Wheel Throw
Aerodynamic Balance	Frise-type nose
Static Balance (Outboard end of each aileron)	Streamlined weight
Trim Tab (Right aileron)	Fixed Bend Tab
Ratio of Aileron Chord to Wing Chord	0.284

HORIZONTAL TAIL DATA

Total Area (Including 2.37 ft.^{2} covered by fuselage)	43.05 ft.^{2}
Span	13.17 ft.
Aspect Ratio	4.02
MAC	3.34 ft.
Airfoil Sections, Root and Tip	NACA 0012
Incidence Angle	-3.0 deg.

ELEVATOR DATA

Total Area	14.10 ft.^{2}
Span	73.58 in.
Deflection	30 deg. up; 20 deg. dwn.
Deflection Trim Tabs (32 in. span, 4-1/2 in. Chord)	±30 deg.
Root Chord	1.5 ft.
Tip Chord	1.0 ft.

TABLE I (continued)

VERTICAL TAIL DATA

Area (Including 2.57 ft.^{2} blanketed by fuselage and excluding 1.84 ft.^{2} dorsal fin area)	12.93 ft.^{2}
Span	4.05 ft.
Airfoil Section	
Root	NACA 0013.2 Modified
Tip	NACA 0012-64 Modified
Incidence Angle (With respect to FRL)	2 deg. Nose Left

RUDDER DATA

Area	6.05 ft.^{2}
Deflection	17 deg. L; 23 deg. R.
Trim Tab	Fixed Bend Tab
Rig (Angle with respect to fin center line)	3 deg. right

FUSELAGE DATA

Fuselage Length Over-all	27.25 ft.
Width, Maximum	4.14 ft.
Depth, Maximum	4.40 ft.
Fineness Ratio	6.2

POWER PLANT DATA

Airplane is powered by one Continental E-185 engine. Maximum continuous rated horsepower at sea level 185 at 2300 RPM.

TABLE I (continued)

POWER PLANT DATA (continued)

The propeller is a Hartzel hydro-selective propeller with the following characteristics:

Activity Factor	100
Diameter	86 in.
Pitch (.75R)	26.5 deg.

MISCELLANEOUS DATA

Weight	
Basic	2129 lbs.
Fuel (40 gal.)	240 lbs.
Pilots (2 with parachutes)	410 lbs.
Gross Weight	2779 lbs.
Center of Gravity Position	29.5% MAC
Tail Length	16.88 ft.
Autopilot Mechanical Gear Ratios	
Deg.Elevator per Deg. Servo-drum	0.919
Deg.Aileron per Deg. Servo-drum	0.910
Deg. Rudder per Deg. Servo-drum	0.330

TABLE II

SPECIFICATIONS OF INSTRUMENTATION COMPONENTS

RATE GYROS

Manufacturer	Minneapolis-Honeywell
Model Number	JG 7005A-24
Power Input	115 volts,400 cycle A.C.
Power Consumption	32 watts (starting), 13 watts (running)
Rotor Speed	20,000 RPM
Weight	1.75 lbs.
Maximum Turn Rate	Modified to approximately 30°/sec.
Potentiometer Resistance	530 ohms
Potentiometer Excitation	Gyro #9 - 24 volts A.C. Gyros #10, #11 and #13 - 30 volts A.C.

SIDESLIP VANE

Manufacturer	Giannini
Model Number	2516
Potentiometer Resistance	1997 ohms
Potentiometer Active Angle	Yaw channel - ± 30° Roll channel- ± 45°
Potentiometer Excitation	Yaw channel - 15 volts A.C. Roll channel- 30 volts A.C.

TABLE II (continued)

TELEMETER TRANSMITTER UNIT

Manufacturer	ASCOP
Model Number	DT-4
Input Signals	0-5 volts D.C.
Information Channels	43 plus two for synchronization of ground station
Sampling Rate	20 RPS
Accuracy	± 1% of full scale
RF Power Output	4 watts
Frequency Range	215-235 MC
Frequency Stability	± 0.05%
Primary Power Requirement	28 volts D.C.
Weight	19.6 lbs.

TABLE III

Dimensional derivatives of the X-15 at Mach = 3.0, $\alpha_o = 10°$

$L_\beta = +9.02$

$L_p = -.212$

$L_r = +.172$

$N_\beta = +2.75$

$N_p = -.00451$

$N_r = -.0451$

$N_{\delta_a} = +.454$

$L_{\delta_a} = +8.40$

TABLE IV

Non dimensional stability derivatives of the X-15 at Mach = 3.0, $\alpha_o = 10°$

$C_{\ell_\beta} = +.044$

$C_{\ell_p} = -.280$

$C_{\ell_r} = +.228$

$C_{n_\beta} = +.315$

$C_{n_p} = -.140$

$C_{n_r} = -1.40$

$C_{n_{\delta_a}} = +.052$

$C_{\ell_{\delta_a}} = +.041$

$C_L = +.440$

$C_{Y_\beta} = -1.38$

TABLE V

Autopilot potentiometer feedback gain constants.

k_4 = +.541 deg. rudder/deg. sideslip

k_5 = -.121 deg. rudder/deg./sec roll rate

k_6 = -.111 deg. rudder/deg./sec yaw rate

k_8 = +.609 deg. aileron/deg. sideslip

k_9 = -.0756 deg. aileron/deg./sec yaw rate

k_7/k_{13} = -.345 deg. rudder/deg. aileron

APPENDIX A

Calculations for the Flight Simulation:

Non-dimensional stability derivatives chosen as typical for the X-15 at M = 3.0, $\alpha_o = 10°$ are:

$C_{\ell_\beta} = + .044$ $\quad C_{n_p} = - .140$ $\quad C_N = C_L = .44$

$C_{\ell_p} = - .280$ $\quad C_{n_r} = - 1.40$ $\quad C_{Y_\beta} = -1.38$

$C_{\ell_r} = + .228$ $\quad C_{n_{\delta a}} = + .052$

$C_{n_\beta} = + .315$ $\quad C_{\ell_{\delta a}} = + .041$

For one - g flight:

$$\rho = \frac{W}{1/2\ C_L\ V^2\ S} = \frac{13,445}{1/2\ (.44)(3 \times 1005)^2(200)} = 3.36 \times 10^{-5} \text{lb-sec}^2/\text{ft}^4 \qquad (1)$$

Where 1005 ft/sec is the speed of sound corresponding to an altitude for which $\rho = 3.36 \times 10^{-5} \text{lb-sec}^2/\text{ft}^4$ (2)

$$q = 1/2 \rho V^2 = 1/2\ (3.36 \times 10^{-5})(9.1 \times 10^6) = 153\ \text{lb/ft}^2 \qquad (3)$$

$$\tau = M/\rho SV = \frac{13,445}{3.36 \times 10^{-5}\ (200)(3015)(32.174)} = 20.6 \qquad (4)$$

$$\mu = M/\rho Sb = \frac{13,445}{3.36 \times 10^{-5}\ (200)(32.174)(22.36)} = 2790 \qquad (5)$$

$$k_x^2 = \frac{I_x}{M} = \frac{3,348}{13,445} \times 32.174 = 8.02\ \text{ft}^2 \qquad (6)$$

$$k_z^2 = \frac{I_z}{M} = \frac{78,691}{13,445} \times 32.174 = 188.4\ \text{ft}^2 \qquad (7)$$

$$J_x = 2\left(\frac{k_x}{b}\right)^2 = 2\ \frac{8.02}{500} = .0321 \qquad (8)$$

$$J_z = 2\left(\frac{kz}{b}\right)^2 = 2\ \frac{188.4}{500} = .753 \qquad (9)$$

Values for dimensional derivatives were obtained as follows:

$$L_\beta = \frac{\mu C_{\ell\beta}}{\tau^2 J_x} = \frac{.044(2790)}{424.4(.0321)} = +\,9.02 \tag{10}$$

$$L_p = \frac{C_{\ell p}}{2\tau J_x} = \frac{-.280}{2(20.6)(.0321)} = -.212 \tag{11}$$

$$L_r = \frac{C_{\ell r}}{2\tau J_x} = \frac{.228}{2(20.6)(.0321)} = +.172 \tag{12}$$

$$N_\beta = \frac{\mu C_{n\beta}}{\tau^2 J_z} = \frac{2790(.315)}{424.4(.753)} = +\,2.75 \tag{13}$$

$$N_p = \frac{C_{np}}{2\tau J_z} = \frac{-\,.14}{2\,(20.6)(.724)} = -.00451 \tag{14}$$

$$N_r = \frac{C_{nr}}{2\tau J_z} = \frac{-\,1.4}{2\,(20.6)(.724)} = -.0451 \tag{15}$$

$$N_{\delta a} = \frac{\mu C_{n\delta a}}{\tau^2 J_z} = \frac{.052(2790)}{424.4\,(.753)} = +.454 \tag{16}$$

$$L_{\delta a} = \frac{\mu C_{\ell\delta a}}{\tau^2 J_x} = \frac{.041\,(2790)}{424.4\,(.0321)} = +\,8.40 \tag{17}$$

The equations which express the relationship between the simulator airplane derivatives and the simulated derivatives are derived in Reference 4. The resultant expressions for the autopilot feedback gain constants are:

$$k_4 = 1.312 - 2.415 \times 10^{-3} L_\beta - 0.2774\,N_\beta \tag{18}$$

$$k_5 = -0.123 - 2.415 \times 10^{-3} L_p - 0.2775\,N_p \tag{19}$$

$$k_6 = -0.124 - 2.415 \times 10^{-3} L_r - 0.2775\,N_r \tag{20}$$

$$k_8 = 0.346 + 0.0490\,L_\beta + 0.0278\,N_\beta \tag{21}$$

$$k_9 = 0.373 + 0.0490\,L_p + 0.0278\,N_p \tag{22}$$

$$k_{10} = 0.0828 + 0.0490\,L_r + 0.0278\,N_r \tag{23}$$

$$\frac{k_7}{k_{13}} = -\frac{20.5(N\delta a/L\delta a) + 0.178}{2.05(N\delta a/L\delta a) + 3.62} \qquad (24)$$

Values obtained, from the foregoing equations, for feedback gain constants were:

k_4 = + .541 deg. rudder/deg. sideslip

k_5 = - .121 deg. rudder/deg/sec roll rate

k_6 = - .111 deg. rudder/deg/sec yaw rate

k_8 = + .609 deg. aileron/deg sideslip

k_9 = + .362 deg. aileron/deg/sec roll rate

k_{10} = - .0756 deg. aileron/deg/sec yaw rate

k_7/k_{13} = - .345 deg. rudder/deg. aileron

Cockpit potentiometer settings were obtained from the calibration curves for these values of feedback gain.

APPENDIX B

The following is a derivation of the root locus equation used to study the effect of pilot gain.

A pilot response, proportional to roll angle, of the form K(1 + .57d) is assumed.

The determinant set, in non-dimensional form, is as follows:

$$\begin{array}{cccc} \underline{\beta} & \underline{d\psi} & \underline{\phi} & \underline{\delta a} \\ C_{Y_\beta} - 2d & -2 & C_L + 2\alpha_o d & 0 \\ \mu C_{l_\beta} & C_{l_r}/2 & \frac{C_{l_p}}{2} d - J_x d^2 & \mu C_{l_{\delta a}} \\ \mu C_{n_\beta} & C_{n_r}/2 - J_z d & \frac{C_{n_p}}{2} d & \mu C_{n_{\delta a}} \\ 0 & 0 & K(1 + .57d) & -1 \end{array} \qquad (1)$$

Expansion of the above can be symbolized in determinental form as:

$$\begin{vmatrix} C_{Y_\beta} - 2d & -2 & C_L + 2\alpha_o d \\ \mu C_{l_\beta} & C_{l_r}/2 & \frac{C_{l_p}}{2} - J_x d^2 \\ \mu C_{n_\beta} & \frac{C_{n_r}}{2} - J_z d & \frac{C_{n_p}}{2} d \end{vmatrix} \qquad (2)$$

$$+ K(1 + .57d) \begin{vmatrix} C_{Y_\beta} - 2d & -2 & 0 \\ \mu C_{l_\beta} & C_{l_r}/2 & \mu C_{l_{\delta a}} \\ \mu C_{n_\beta} & C_{n_r}/2 - J_z d & \mu C_{n_{\delta a}} \end{vmatrix} = 0$$

Expansion of the first determinant set will yield a quartic equation which can be divided by $2J_xJ_z$ and then factored into a form from which the characteristic modes of transient motion can be deduced. Thus this is the characteristic equation and will be symbolized as:

$$|D| = (\lambda+\lambda_R)(\lambda+\lambda_S)(\lambda^2 + 2\zeta_\psi\omega_{n\psi} + \omega_{n\psi}^2) \tag{3}$$

The remaining determinant can be expanded and the sum represented as follows:

$$|D| + \frac{K(1+.57d)}{2J_xJ_z}\left\{\mu C_{l\delta a}\left[(C_{Y\beta}-2d)\left(\frac{C_{nr}}{2}-J_z d\right) + 2\mu C_{n\beta}\right] - \mu C_{n\delta a}\left[(C_{Y\beta}-2d)\frac{C_{lr}}{2} + 2\mu C_{l\beta}\right]\right\} \tag{4}$$

This can be rearranged to yield:

$$|D| + K(1+.57d)\frac{\mu C_{l\delta a}}{J_x}\left\{\left[d^2 - \frac{(C_{nr}+J_zC_{Y\beta})d}{2J_z} + \frac{C_{Y\beta}\frac{C_{nr}}{2}+2\mu C_{n\beta}}{2J_z}\right] + \frac{C_{n\delta a}}{C_{l\delta a}}\frac{C_{lr}}{2J_z}\left[d - \left(\frac{C_{Y\beta}}{2} + \frac{2\mu C_{l\beta}}{C_{lr}}\right)\right]\right\} \tag{5}$$

The terms multiplying the human transfer function are seen to be a quadratic which is known to yield a complex pair of roots. Accordingly the above may be symbolized as follows: (d is replaced by λ)

$$|D| + \frac{\mu C_{l\delta a}}{J_x}K(1+.57\lambda)(\lambda^2 + 2\zeta_\phi\omega_{n\phi} + \omega_{n\phi}^2) \tag{6}$$

The root locus equation is thus found to be:

$$\frac{(\lambda+\lambda_R)(\lambda+\lambda_S)(\lambda^2 + 2\zeta_\psi\omega_{n\psi}\lambda + \omega_{n\psi}^2)}{(\lambda^2 + 2\zeta_\phi\omega_{n\phi}\lambda + \omega_{n\phi}^2)(1+.57\lambda)} + \frac{\mu C_{l\delta a}}{J_x}K = 0 \tag{7}$$

APPENDIX C

Discussion of Phasing of Roll and Sideslip:

One of the parameters discussed in conjunction with the instability studied herein is the phase relation of roll angle and sideslip angle. This relationship is the subject of the following discussion.

From the basic determinant for the lateral-directional motion of the airplane, given here in Laplace operator form as:

$$\begin{array}{cccc}
\beta & d\psi & \phi & \delta_a \\
C_{Y_\beta} - 2s & -2 & C_L + 2\alpha_0 s & 0 \\
\mu C_{l_\beta} & \frac{C_{l_r}}{2} & \frac{C_{l_p}}{2}s - J_x s^2 & -\mu\frac{C_{l\delta_a}}{s} \\
\mu C_{n_\beta} & \frac{C_{n_r}}{2} - J_z s & \frac{C_{n_p}}{2}s & -\mu\frac{C_{n\delta_a}}{s}
\end{array} \tag{1}$$

one may form the ratio ϕ to β as:

$$\frac{\phi}{\beta} = \frac{\begin{vmatrix} C_{Y_\beta} - 2s & -2 & 0 \\ \mu C_{l_\beta} & \frac{C_{l_r}}{2} & -\mu\frac{C_{l\delta_a}}{s} \\ \mu C_{n_\beta} & \frac{C_{n_r}}{2} - J_x s & -\mu\frac{C_{n\delta_a}}{s} \end{vmatrix}}{\begin{vmatrix} 0 & -2 & C_L + 2\alpha_0 s \\ -\mu\frac{C_{l\delta_a}}{s} & \frac{C_{l_r}}{2} & \frac{C_{l_p}}{2}s - J_x s^2 \\ -\mu\frac{C_{n\delta_a}}{s} & \frac{C_{n_r}}{2} - J_z s & \frac{C_{n_p}}{2}s \end{vmatrix}} \tag{2}$$

This may be written as:

$$\phi/\beta = \frac{s^2 + A\,s + B}{C\,s^2 + D\,s + E} \tag{3}$$

where

$$A = \frac{C_{n\delta a}}{C_{l\delta a}}\,\frac{C_{lr}}{2J_z} - \frac{C_{Y\beta}}{2} - \frac{C_{nr}}{2J_z}$$

$$B = \frac{\mu C_{n\beta}}{J_z} + \frac{C_{Y\beta}C_{nr}}{4J_z} - \frac{C_{n\delta a}}{C_{l\delta a}}\,\frac{C_{lr}}{2J_z}\left(\frac{C_{Y\beta}}{2} + \frac{2\mu C_{l\beta}}{C_{lr}}\right)$$

$$C = 2J_x\,\frac{C_{n\delta a}}{C_{l\delta a}} - 2\alpha_o J_z$$

$$D = C_{np} - C_L J_z + \alpha_o C_{nr} - \frac{C_{n\delta a}}{C_{l\delta a}}\left(C_{lp} + \alpha_o C_{lr}\right)$$

$$E = \frac{C_L C_{nr}}{2} - \frac{C_{n\delta a}}{C_{l\delta a}}\,\frac{C_L C_{lr}}{2}$$

For the condition of low dynamic pressure (153 lb/ft^2), with $\alpha_o = 10°$ this ratio can be written

$$\frac{\phi}{\beta} = \frac{s^2 + 1.81s + 962.1}{-.182s^2 - .366s - .3716} \quad \text{or} \tag{4}$$

$$\frac{\phi}{\beta} = \left[\frac{s + .91 \pm 31.0\,j}{s + 1.01 \pm .957\,j}\right] \text{Constant}$$

These roots are plotted on the complex plane and yield a phase relation for ϕ/β of -173 degrees (Fig. 20).

It appears from an examination of the above expression of ϕ/β that in those cases where the Dutch roll mode is lightly damped, the damping terms of the numerator and

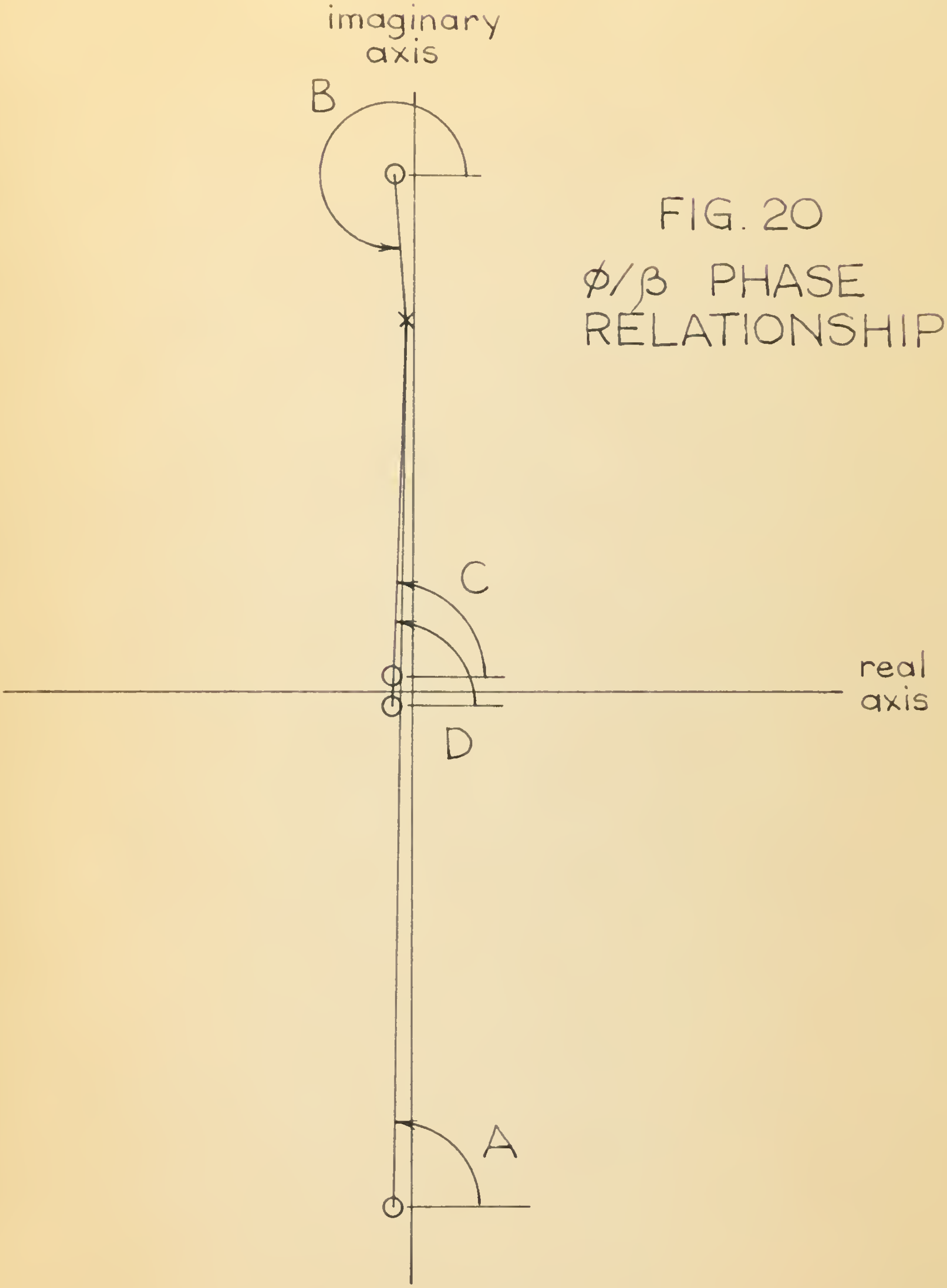

FIG. 20

ϕ/β PHASE RELATIONSHIP

$$\phi/\beta \text{ PHASE} = \angle A + \angle B - \angle C - \angle D$$
$$= -173°$$

denominator will also be small. This means that all the roots will lie close to the imaginary axis. Further, by analyzing the plot of these roots, it is evident that the phasing of the ϕ/β motion is primarily dependent upon the relative position of the numerator root and the Dutch roll root. If the numerator root has an imaginary part greater than the imaginary part of the dutch roll root, the phasing between ϕ and β will be approximately 180 degrees. If the Dutch roll imaginary part is the larger, then the phasing will be nearly zero degrees.

Those parameters which affect the imaginary part of the Dutch roll root are difficult to isolate since all approximations applied to the condition under investigation yielded poor results. However, it is evident that a major contribution comes from $\frac{\mu C_{n\beta}}{J_z}$. This combination of parameters also appears in coefficient B in the expression for ϕ/β, so its influence in shifting the two roots is equal. The only other significant term in coefficient B is $-2\mu C_{l\beta}\frac{C_{n\delta a}}{C_{l\delta a}}$. It is through this expression that a major shift in the numerator root is achieved. In the case under consideration, this one term is large enough to shift the numerator root below the Dutch roll root, changing the phasing to zero degrees. This shift would occur if one of the three parameters had a sign change.

This is merely additional supporting evidence for the argument that the phase relation between ϕ and β, and the yaw due to aileron are important parameters in the explanation of pilot induced lateral-directional instabilities. It also points out the problem which will arise in any airplane - pilot combination where C_{l_β} changes sign within the performance envelope. If this change of sign occurs in an area where other conditions are favorable to pilot-induced instabilities, then these instabilities may well be encountered.

APPENDIX D

Discussion of Dutch Roll to Roll Mode Phasing:

In an attempt to shed more light on the mechanism producing the type of instability under consideration, the following analysis of Dutch roll to roll mode was made. Of particular interest was the phase relation of the two motions.

Again the basic determinant for the lateral-directional motion of the airplane is given here in Laplace operator form.

$$\begin{array}{cccc}
\beta & d\psi & \phi & \delta a \\
C_{Y\beta} - 2s & -2 & C_L + 2\alpha_0 s & 0 \\
\mu C_{l\beta} & \frac{C_{lr}}{2} & \frac{C_{lp}}{2}s - J_x s^2 & -\mu C_{l\delta a} \\
\mu C_{n\beta} & \frac{C_{nr}}{2} - J_z s & \frac{C_{np}}{2}s & -\mu C_{n\delta a}
\end{array}$$

Forming an expression for $\dot{\phi}$ in terms of this determinant and applying a step input yields the following determinant for $\dot{\phi}$.

$$\dot{\phi} = \frac{\begin{vmatrix} C_{Y\beta} - 2s & -2 & 0 \\ \mu C_{l\beta} & C_{lr}/2 & -\mu C_{l\delta a} \\ \mu C_{n\beta} & \frac{C_{nr}}{2} - J_z s & -\mu C_{n\delta a} \end{vmatrix}}{\begin{vmatrix} C_{Y\beta} - 2s & -2 & C_L \\ \mu C_{l\beta} & C_{lr}/2 & \frac{C_{lp}}{2}s - J_x s^2 \\ \mu C_{n\beta} & \frac{C_{nr}}{2} - J_z s & \frac{C_{np}}{2}s \end{vmatrix}}$$

This may be written as:

$$\dot{\phi} = \frac{A\left(s^2 + Bs + C\right)}{(s-\lambda_1)(s-\lambda_2)(s-\lambda_3)(s-\lambda_4)}$$

where

$$A = \mu \frac{C_{l\delta a}}{J_x}$$

$$B = \frac{C_{l_r}}{2J_z} \frac{C_{n\delta a}}{C_{l\delta a}} - \frac{(C_{n_r} + J_z C_{Y\beta})}{2J_z}$$

$$C = \frac{(C_{Y\beta} C_{n_r}/2) + 2\mu C_{n\beta}}{2J_z} - \frac{C_{l_r}}{2J_z} \frac{C_{n\delta a}}{C_{l\delta a}} \left(\frac{C_{Y\beta}}{2} + \frac{2\mu C_{l\beta}}{C_{l_r}} \right)$$

and the denominator represents the characteristic of motion.

For the condition of low dynamic pressure (153 lb/ft^2) with $\alpha_o = 10°$, this expression becomes:

$$\dot{\phi} = \frac{3565(s^2 + 1.814s + 961)}{(s-\lambda_1)(s-\lambda_2)(s-\lambda_3)(s-\lambda_4)}$$

The roots of the above are plotted on the complex plane (Fig. 21). It can be seen that the phase angle changes by 180 degrees whenever the numerator root moves inside the Dutch roll root. Further, a comparison of the roll traces (Figs. 9 and 16) shows the same result. Figure 9, with effective adverse yaw, shows a time delay of 1.5 seconds to reach the first peak on the roll trace. Figure 16, with the same conditions except effective proverse yaw, shows a time delay of .5 seconds. This difference in time corresponds to one half the period of the Dutch roll motion. Here again, as in the ϕ to β relation, we observe a change in phase of 180 degrees at the same point where ω_ϕ/ω_ψ becomes greater than 1.

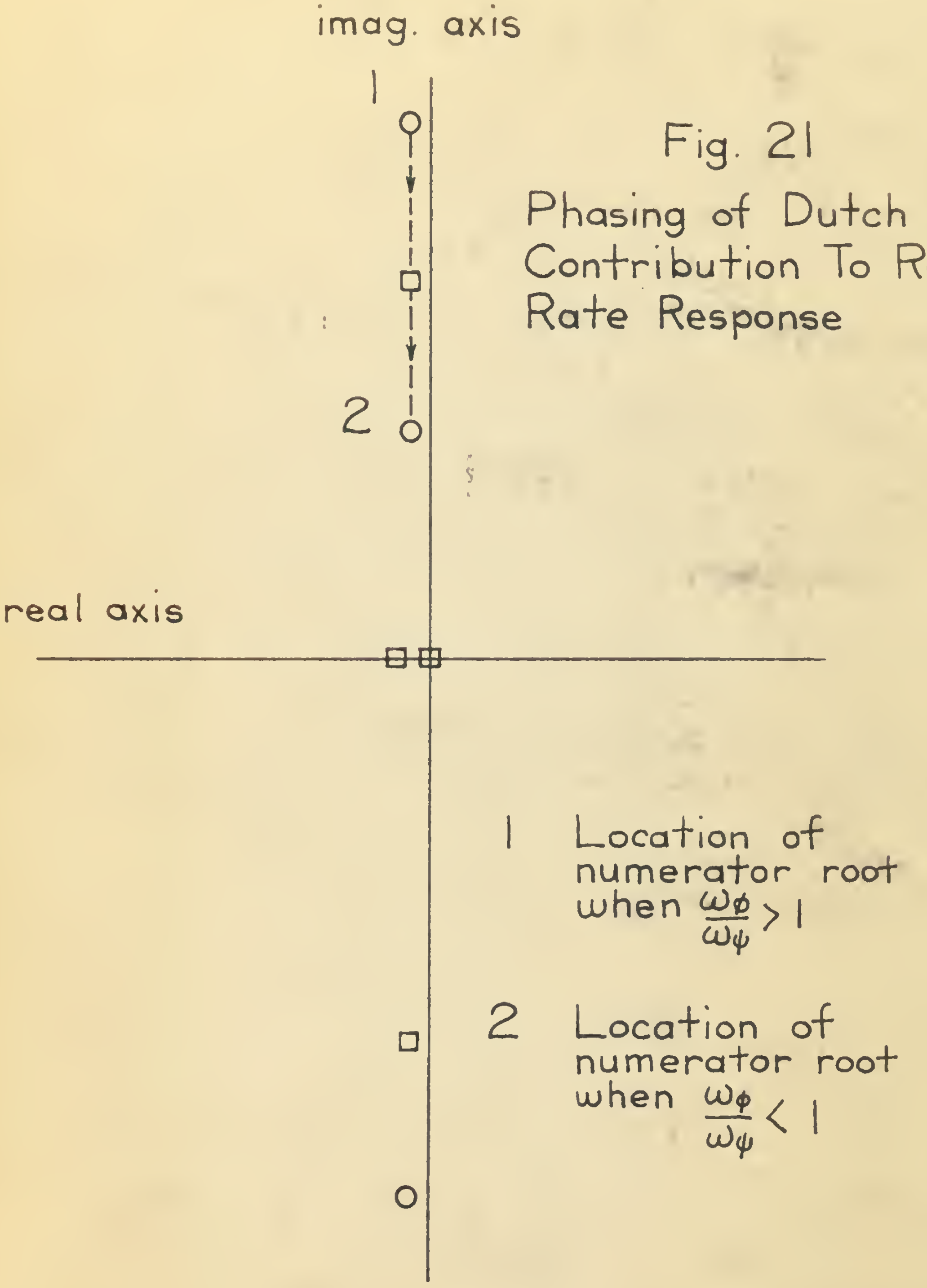

Fig. 21

Phasing of Dutch Roll Contribution To Roll Rate Response